COMPARATIVE STUDY OF THIN FILM DEPOSITION AND CHARACTERIZATION USING CARBONIC MATERIALS

by

ABDULLA ALL MAHMUD

AHSANUL ISLAM SIKDER

BACHELOR OF SCIENCE IN ELECTRICAL AND ELECTRONIC ENGINEERING

Department of Electrical and Electronic Engineering
INTERNATIONAL ISLAMIC UNIVERSITY CHITTAGONG

December 2021

COMPARATIVE STUDY OF THIN FILM DEPOSITION AND CHARACTERIZATION USING CARBONIC MATERIALS

by

ABDULLA ALL MAHMUD

AHSANUL ISLAM SIKDER

A thesis
submitted as partial fulfilment of the requirement for the degree of

BACHELOR OF SCIENCE IN ELECTRICAL AND ELECTRONIC ENGINEERING

Department of Electrical and Electronic Engineering
INTERNATIONAL ISLAMIC UNIVERSITY CHITTAGONG

December 2021

CERTIFICATE OF APPROVAL

The thesis entitled as "**Comparative Study of Thin Film Deposition and Characterization Using Carbonic Materials**" submitted by **Abdulla All Mahmud**, bearing Matric ID. **ET-171016** and **Ahsanul Islam Sikder**, bearing Matric ID. **ET-171013** of session **Spring 2017**, to the Department of Electrical and Electronic Engineering, International Islamic University Chittagong, has been accepted as satisfactory in partial fulfilment of the requirements for the degree of Bachelor of Science in Engineering and approved for the examination held on **24th December, 2021**.

_____

Supervisor
Muhammad Athar Uddin
Associate Professor
Department of Electrical and Electronic Engineering
International Islamic University Chittagong.

DECLARATION

It is hereby declared that this work has been done by us and no portion of the work contained in this thesis has been submitted elsewhere for the award of any degree or diploma.

_____

Abdulla All Mahmud

_____

Ahsanul Islam Sikder

ACKNOWLEDGMENT

All praises and thanks to Allah, the Lord of the world, the most Beneficent, the most Merciful for helping us to accomplish this work.

We are beholden to a number of people, who supported us to carry out this work. We would like to express our profound gratitude to our Supervisor Muhammad Athar Uddin, Associate Professor, Department of Electrical & Electronic Engineering, International Islamic University Chittagong for immense guidance and supervision in this thesis. We are very grateful to him for his valuable time to make our thesis successful. We also extend our gratitude to all the teachers of the Department of Electrical and Electronic Engineering of International Islamic University Chittagong. Very special thanks to our family members. Words cannot express how grateful we are to our parents.

Authors

ABSTRACT

Electrolysis of methanol with Camphor and CNT was used to deposit carbon thin films on Aluminum (Al), Copper (Cu), Silicon (Si), Zinc (Zn) substrates and CNT materials were used to spin coat Silicon (Si). The integration of camphor ($C_{10}H_{16}O$), a natural source in methanol is studied. To make the electrolytes, different amounts of camphor were combined in methanol solvent. On the negative electrode Al, Cu, Si and Zn substrates were placed. With increasing camphor concentration, the volatility of current density as a function of applied voltage shifted significantly. It is discovered that the current density of all substrates drops initially with camphor compared to a methanol solution and then increases. However, the amount of camphor that can be added to a methanol solution to increase current density has a limit. The amount of camphor needed to achieve maximal current density was found to vary depending on the substrate. On the Zn substrate, the maximum current density was recorded during camphor deposition. CNT deposition on Si substrate produced higher current densities than camphor. The P^H of several solutions was measured before and after deposition. Camphor has a P^H altering effect. Variations in P^H were found as the amount of carbonic materials in the methanol solution varied. Changes in PH before and after deposition indicate any chemical changes on the substrates. The films were examined using scanning electron microscopy (SEM) and energy dispersive X-ray spectroscopy (EDS). Sharp variations between deposited films can be seen in EDS and SEM micrographs. In SEM, the effects of Methanol and other carbonic materials can be seen. In terms of SEM analysis spin coating shows better nano properties compared to electrodeposition. When comparing nano carbonic materials to camphor, EDS research showed that the carbon percentage of the electrodeposited films is higher for nano carbonic materials. The largest percentage of carbon was detected in films made with MWCNT on Si substrate (both electrodeposition and spin coating).

TABLE OF CONTENTS

LIST OF FIGURES

LIST OF TABLES

LIST OF ABBREVIATIONS

CNT	-	Carbon Nanotubes
SWNT	-	Single-walled Nanotubes
MWNT	-	Multi-walled Nanotubes
SWCNT	-	Single-walled Carbon Nanotubes
MWCNT	-	Multi-walled Carbon Nanotubes
DLC	-	Diamond-liked Carbon
SEM	-	Scanning Electron Microscopy
EDS	-	Energy Dispersive X-ray Spectroscopy
PLD	-	Pulsed Laser Deposition
CVD	-	Chemical Vapour Deposition
MIS	-	Metal Insulator Semiconductor
TFT	-	Thin Film Transistor
IBS	-	Ion-beam-sputtering
CC	-	Camphoric Carbon
LEED	-	Low-energy Electron Diffraction
PD	-	Plasma Deposition
PACVD	-	Plasma-assisted Chemical Vapour Deposition
RF	-	Radio Frequency
CRT	-	Cathode Ray Tube
TEM	-	Transmission Electron Microscopy
FTIR	-	Fourier-transform Infrared Spectroscopy
UV-VIS-NIR	-	Ultraviolet Visible Near Infrared Spectroscopy

CHAPTER 1
INTRODUCTION

1.1 Introduction

In the semiconductor industry, silicon (Si) and other compound semiconductor-based materials have long been employed. It has a diverse variety of structural, mechanical, optical, and electrical characteristics. Carbon has attracted the interest of researchers and engineers looking for alternative low-cost materials for use in electronic device production and solar cells. Carbon can be found in nature in a variety of forms, ranging from graphite to diamond, each with its own set of characteristics. Aside from these, carbon can be found in nature in a variety of amorphous forms. The device researchers are now very interested in these amorphous forms of carbon.

Fullerenes, which were long considered exotic are now frequently produced and employed in study thanks to recent developments in the science of crystalline carbon. Among them are bucky balls (C_{60}), single-walled carbon nanotubes (SWCNT), multi-walled carbon nanotubes (MWCNT), carbon nano fibres and other materials. Carbon films' Optical and electrical characteristics are mostly determined by the precursors and deposition technique. As a result, researchers working on alternate precursor materials and easy deposition methods have been given top emphasis. As an alternate precursor material, mixed fullerene (C_{60} and C_{70}), MWCNT and SWCNT have been used individually in this study.

From the previous works of carbon thin film deposition, The Electroplating and Spin coating process with methanol was used to try carbon thin film deposition (CH_3OH). Methanol was used to include camphor ($C_{10}H_{16}O$), mixed fullerene (C_{60} and C_{70}), carbon nanotubes (multi-walled and single-walled), and graphite. To make the solution, different concentrations of camphor and carbon compounds were combined with methanol. Al, Cu, Zn and Si substrates were used for the deposition. The results from the previous works have been compared here and a number of characteristics have been investigated.

1.2 Background

The discovery of a third allotrope of carbon, the fullerene molecule's molecular crystal, 'buckyball' C_{60}, and the finding that diamond may be easily created by vapour deposition were both major breakthroughs in the study of crystalline carbon [1]. In disordered carbons, A commensurate increase in effort has occurred. Soots, chars, carbon fibres, glassy carbon and evaporated amorphous carbon are examples of disordered carbons. In the most fundamental sense, these carbons are sp^2 linked. Amorphous carbon (a-C) and hydrogenated amorphous carbon (a-C: H) have been developed that are physically stiff, infrared transparent and chemically inert using a variety of unique synthesis processes. They're currently being used as antireflective coatings for infrared windows and as hard coating materials for magnetic disc drives. The sp^3 component of their bonding is responsible for their advantageous qualities and these carbons are usually referred to as diamond-like carbons (DLC). This form of carbon may be totally amorphous or have crystalline inclusions. On a more fundamental level, materials scientists, as well as solid-state chemists and physicists, are interested in non-crystalline carbons.

Carbon films' optical and electrical characteristics are mostly determined by the precursors and deposition technique. As a result, In order to generate a carbon thin film with the requisite optical and electrical characteristics for usage in a range of opto-electronic devices, these two parameters are carefully assessed. As a result, the focus has turned to simpler deposition techniques and alternative precursor materials. Camphor ($C_{10}H_{16}O$) was found as an alternate precursor material in this study because it has some advantages over graphite [2].

Camphor's structure contains both sp^2 and sp^3 hybridized carbon, whereas graphite is fully sp^3 hybridized. Hydrogen in a-C films changes their characteristics and introduces a lot of sp^3 sites. The dangling bond in the gap states is passivated by hydrogen, which also tailors the film's optoelectronic properties. Extra hydrogen gas / ions must be given to employ graphite as a precursor, although camphor has a lot of hydrogen in its composition. Camphor molecules with sp^3-hybridized bonds help produce carbon films, particularly diamond-like carbon (DLC) films.

In the sp^2 hybridization, elemental carbon can take on a variety of interesting shapes. Carbon may form closed and open cages with honeycomb atomic arrangement in addition to the well-known graphite. With the C_{60} molecule, Kroto et al. were the first to discover such a structure [3]. Despite the fact that various carbon cages had been studied, Iijima was the first to develop tubular carbon structures in 1991 [4]. The nanotubes were made up of tens of graphitic shells spaced by 0.34 nanometers. with widths of 1 nanometers and a significant length/diameter ratio (so-called multi-walled carbon nanotubes (MWNTs)). Two years later, Iijima and Ichihashi and Bethune et al created single-walled carbon nanotubes (SWNTs) [5],[6]. In today's world, three processes are employed to create MWNTs and SWNTs: arc discharge, laser ablation, and catalytic growth. Raman, electrical, and optical spectroscopies are used to characterize the produced nanotube samples. Mechanical, electrical, and thermal measurements provide valuable information. Progress in nanotube use is being made in tandem with advancements in nanotube synthesis and characterisation techniques. The nanotubes' high Young's modulus and tensile strength have generated interest in their use in composite materials with improved mechanical characteristics [7]. Because of their nanosize, structural perfection, high electrical conductivity, and chemical durability, nanotubes are ideally suited as electron field emitters for use in flat panel displays [8].

1.3 Objectives of the Work

The following are the work's objectives:

- Characterization and comparative study of carbon thin film deposition by different methods using different carbonic materials on different substrates.
- Preparing a summary of works of carbon thin film deposition.

1.4 Purpose of choosing Carbon

- For many years, Si and some compound semiconductors have dominated the semiconductor industry.
- Alternative low-cost materials are being sought by researchers.
- Carbon has tunable Opto-Electronic Properties.
- Carboneous film research and gadgets based on carbon thin films are gaining popularity.

1.5 Purpose of choosing CNT

- Nanotubes are composed entirely of sp^2 bonds.
- SWCNT is conducting or semiconducting as per rolling.
- MWCNT is concentric SWCNTs with different diameters.
- Fullerene can be dissolved in common solvent.
- The properties of CNT are tunable.
- CNT based carbonic thin film may have higher conductivity.

1.6 Thesis Layout

The thesis is divided into five chapters.

The **First Chapter** discusses the work's history and purpose.

Carbon materials, diverse forms of carbon, and the current state of carbon research are covered in **Chapter Two** as are thin films, their history and applications. Several types of deposition processes will also be discussed in this chapter (such as ion beam methods, sputtering, plasma deposition, electroplating).

The methodology and experimental specifics of carbon thin film deposition, SEM, and EDS analysis are covered in **Chapter Three.**

The **Fourth Chapter** summarizes the work done on carbon thin film deposition, including results and discussions on the deposition process, as well as certain characteristics of carbon thin films generated during electrolysis of organic solutionsare. Previous work's experimental results have been compared. Previous work's EDS and SEM testing results were used to investigate the films deposited in various solutions.

The final views and discussions are included in **Chapter Five**. There are also some suggestions for future scope of work included here.

CHAPTER 2
REVIEW ON THIN FILM DEPOSITION

2.1 Introduction to Carbon Material

Carbon is found in crystalline and amorphous solids in its elemental form all throughout the world. The two crystalline allotropes of carbon are diamond and graphite. With interatomic lengths of 0.15mm, Diamond has a face-centered cubic crystal structure. Each carbon atom has four other carbon atoms with which it is covalently linked (sp^3 tetragonal bonds). In the basal plane, carbon atoms are organized in layers with strong trigonal bonds (sp^2) and an inter-atomic spacing of 0.1415nm. The fourth electron in the outer shell produces a weak Vander Walls connection between planes, explaining graphite's superior electrical conductivity, lubricity, decreased density, grayish black color and softness as opposed to diamond's.

The graphite phase with strong in plane trigonal bonding is a stable state under ambient circumstances. At high pressure and temperature, irradiation or heat can convert graphite to diamond; however, when subjected to irradiation or heat, diamond quickly transforms back to the more stable graphite phase. During the fabrication of a diamond thin film, it is observed that diamond structure occurs only under very particular conditions, whereas graphite structure prevails in all other cases.

Carbon's distinctive properties (especially diamond-like carbon) and the demand for current technologies, particularly those related to advancements in the electronics industry, have stimulated interest in creating thin carbon films (especially diamond-like carbon). Extreme hardness, chemical inertness, high electrical resistivity, high dielectric strength, optical transparency, and thermal conductivity are among these qualities. These are a few techniques for producing high-quality diamond-like carbon (DLC) thin films. This chapter discusses the current state of amorphous and diamond-like carbon studies.

2.2 Various Form of Carbon and Carbon Nano Materials

Carbon is found in Group IV and has an atomic number of 6 of the second periodic table, with the electronic ground state configuration $1s^2 2s^2 2px^1 2py^1$ as seen in **Fig. 2.1**.

The four electrons in the outer orbital can form distinct hybridized bonding configurations by arranging themselves in different combinations of outer shell sub orbitals (S, Px, Pz) (sp^1, sp^2, sp^3). 1 The trigonal (sp^2) or tetrahedral (sp^3) arrangements determine the structure of graphite or diamond.

Aside from graphite and diamond, a variety of carbon-based materials can be classified as imperfect diamond structures because their layers are not aligned with their common axis, their angular displacement is random and their layers overlap unevenly.

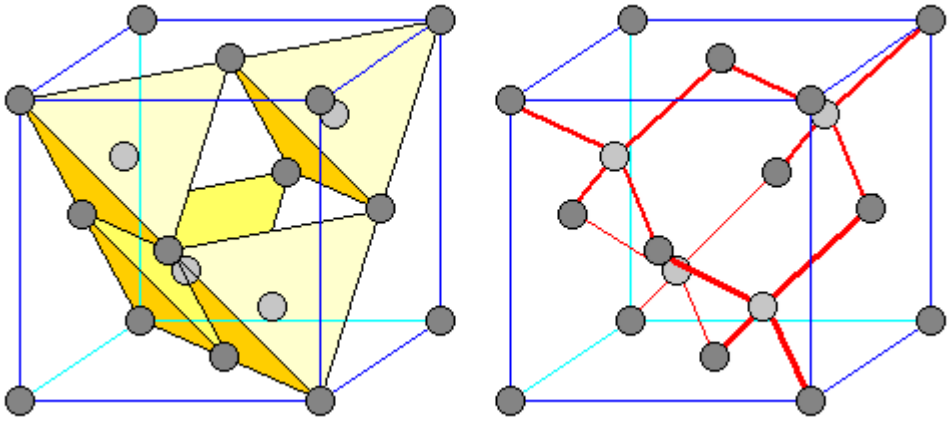

Fig. 2.1 The ideal diamond structure [35]

The quantity of sp^2 and sp^3 linked carbon in certain essential kinds of carbon (DLC), amorphous carbon (a-C), and hydrogenated amorphous carbon (HA-C) varies (a-C:H). Scientists from all around the world began investigating carbon and carbon-related materials, particularly a-C or a-C: H, for application in optoelectronic devices soon after the fooleries family was discovered in 1985.

2.2.1 Fullerene:

Fullerenes are enormous carbon clusters with a closed cage that exhibit a number of unique features not found in any other chemical as seen in **Fig. 2.2**. As a result, fullerenes are an intriguing chemical class that will likely find use in future technologies and applications. Before the smaller fullerenes C_{60} and C_{70} were discovered, it was commonly considered that these massive spherical molecules were unstable.On the other hand, several Russian scientists have discovered that C_{60} in the gas phase was stable and had a high band gap. Fullerenes, like many other key scientific discoveries, were found by chance. In 1985, Kroto and Smalley discovered

some unexpected results in the mass spectra of evaporated carbon samples.Fullerenes were discovered here and their stability in the gas phase was demonstrated. The hunt for more fullerenes has begun. Since Iijima and colleagues discovered carbon nanotubes in 1991, A huge number of researchers from all around the world have looked into them. Their vast length (up to several microns) and small diameter result in a huge aspect ratio (a few nanometers).

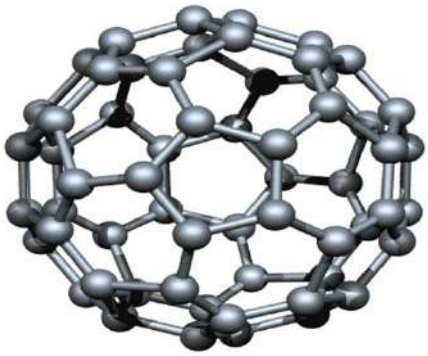

Fig. 2.2 The Structure of Fullerene [36]

2.2.2 SWCNT and MWCNT:

Fullerenes come in a variety of unique shapes, including typical spheres, cones, tubes, and more intricate and bizarre geometries. Here, we'll go through some of the most well-known and important structures. Long wrapped graphene sheets are what Single Walled Nanotubes (SWNT) are. Nanotubes have a length-to-diameter ratio of about 1000, making them nearly one-dimensional structures.

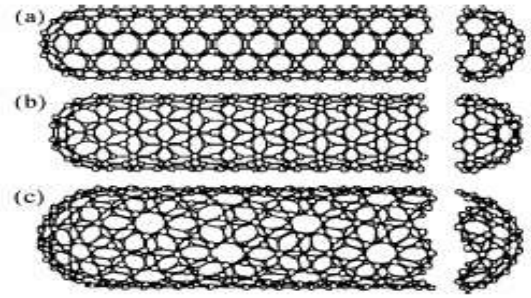

Fig. 2.3 Some SWNTs with different chiralities. At the open end of the tubes, the structural difference is plainly visible. a) Armchair structure b) zigzag structure c) chiral structure [37]

Two discrete zones with different physical and chemical properties make up a SWNT. The tube's sidewall is the first, and the tube's end cap is the second. The end cap

structure is similar to or derived from that of a smaller fullerene like C_{60}. C atoms are organized in hexagons and pentagons in end cap formations. It is easy to derive from according to Euler's theorem, a closed cage construction made entirely of pentagons and hexagons requires a total of twelve pentagons. The requisite curvature of the surface to enclose a volume is created by combining a pentagon with five surrounding hexagons. According to the isolated pentagon rule, the distance between pentagons on the fullerene shell should be raised to achieve the least amount of local curvature and surface tension, resulting in a more stable structure. The smallest stable structure that can be created in this manner is C_{60}, which is followed by C_{70} and so on. Another feature of fullerenes is that they all have an even number of C-atoms, as adding one hexagon to an existing structure adds two C-atoms. A cylinder is the other structure that makes up a SWNT. When a graphene sheet of a given size is coiled in a specific direction, it produces it.

We can only roll in a finite number of directions to produce a closed cylinder since the outcome is cylinder symmetric in **Fig. 2.4.** The origin is chosen to be one of the atoms in the graphene sheet. Roll the sheet until the two atoms are in the same location. The chiral vector is a vector that points from the first to the second atom and has the same length as the circumference of the nanotube in **Fig. 2.3.** The chiral vector is perpendicular to the axis of the nanotube. Optical activity, mechanical strength, and electrical conductivity of SWNTs with different chiral vectors vary.

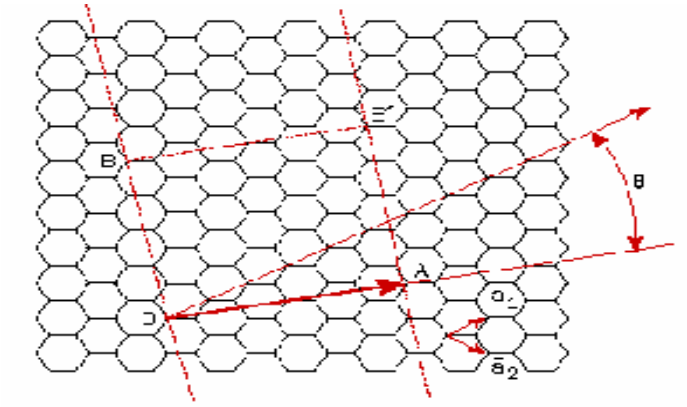

Fig. 2.4 The chiral vector is the OA vector. The vector Ch=na1+ma2 and the chiral angle _with the zigzag axis may be used to define it. The lattice vectors are vectors a1 and a2 [38]

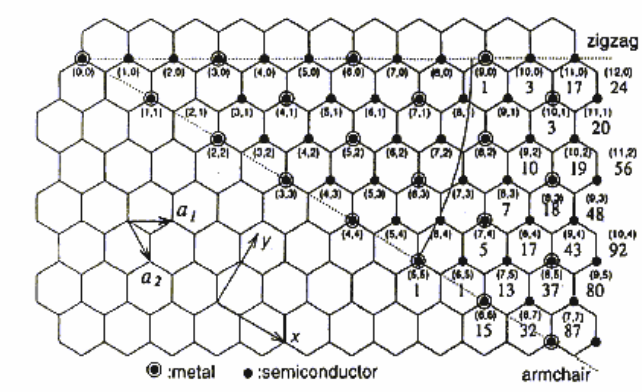

Fig. 2.5 All potential SWNT structures can be created using chiral vectors in the range shown in this diagram. (n, m), where n and m are integers and m<=n or _<30º [39]

We analyze possibly desirable or undesirable defects after discussing ideal architectures without flaws.

By replacing a hexagon with a heptagon or pentagon, deformations such as bends and nanotube connections can be introduced. Deformations can be inward or outward, and they have a significant impact on electrical characteristics, among other things. Impurities introduced during or after the nanotube growth process generate another type of defect; compounds that can be integrated into the structure include catalyst particles, for example.

Multi Walled Nanotubes (MWNT) can be thought of as a collection of concentric SWNTs of various sizes. These structures differ greatly in length and diameter from those previously mentioned.

Their qualities, of course, are vastly different in **Fig. 2.6**.

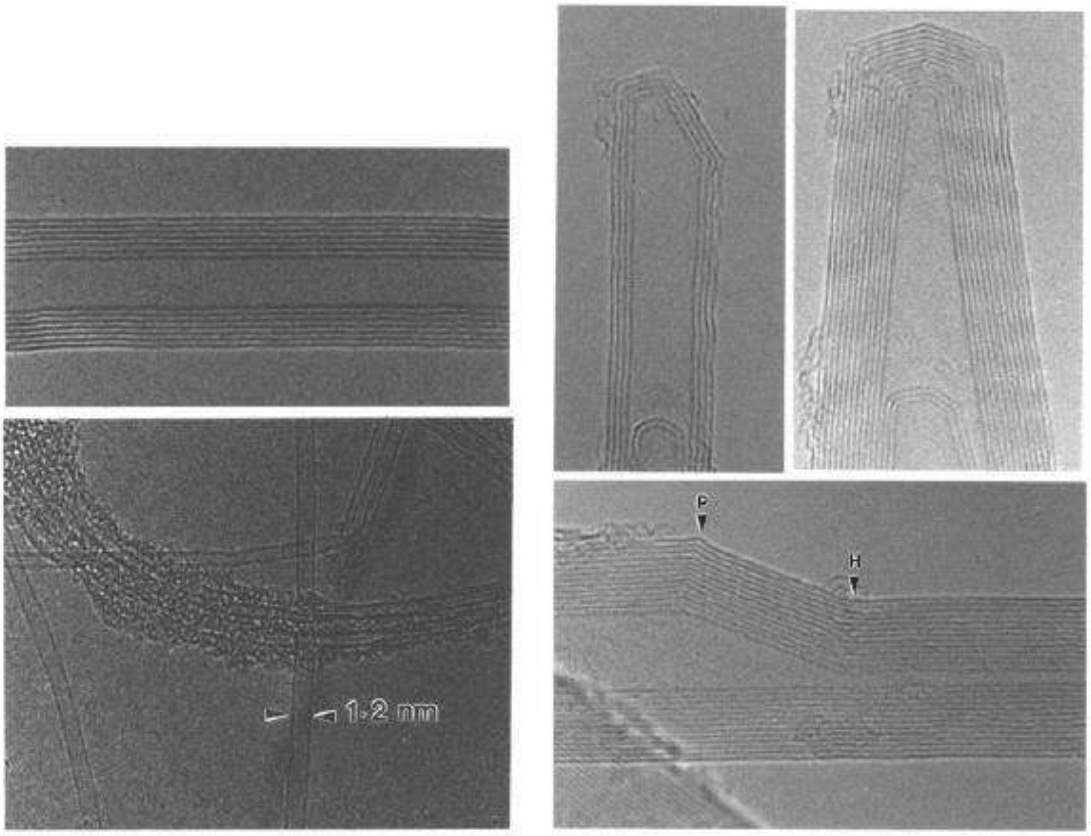

Fig. 2.6 Different structures of MWNTs. A cross-section of a MWNT is shown at the top left. The multiple walls are clearly visible, separated by 0.34nm. The MWNT is obtained by rotating around the symmetry axis. Top-right: MWNT end caps with symmetrical or asymmetrical cone shapes. A SWNT with a diameter of 1.2nm and a bundle of SWNTs covered with amorphous carbon are shown at the bottom left. Bottom-right: A MWNT with flaws. There is a pentagon flaw in point P and a heptagon defect in point H [40]

Carbon cones are also depicted in **Fig. 2.6**. It can be thought of as a progressive transition from a big to a smaller diameter, with no faults in the cone wall but fewer pentagons in the end cap.

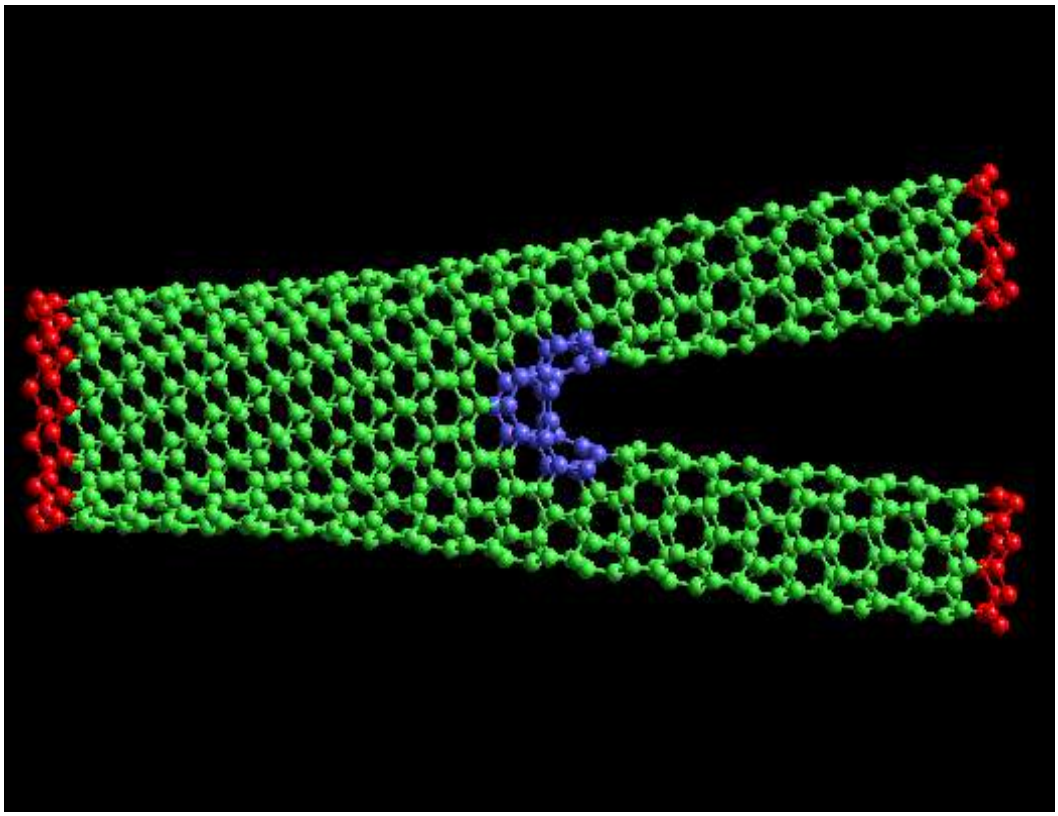

Fig. 2.7 Left: The faults are marked in blue on a Y-branch. Right: A metallic to semiconducting SWNT transition. Pentagons and heptagons are inserted to make the change [41]

Defects can also lead to the formation of novel structures like as Y-branches, T-branches, and SWNT junctions in **Fig. 2.7**. Under some situations, these flaws can be introduced in a 'controlled' manner. 7 These flaws result in unique structures with different, but equally intriguing, features than their original forms. Defects are being researched as well, but they will not be addressed in this study. Another noteworthy structure is peapods, which are carbon nanotubes with C_{60} molecules encapsulated within the nanotube.

2.3 Present Status of Carbon Research

A carbon network with sp^2 and sp^3 bonding structures is known as amorphous carbon but no sp^1 bonding. Many researchers have recently indicated an interest in combining diamond-like carbon (DLC) and a-C film to create microelectronic devices. Carbon can be changed across an extremely large range, from semi-metallic graphite (0.0 eV) to insulating diamond, thanks to the many distinctive features of DLC, a-C, or a-C: H. (5.5 eV.). Growth conditions, deposition techniques, and precursor materials all have an

impact on these properties. To create a-C or a-C:H films, many processes such as pulsed laser deposition (PLD), ion beam deposition (IBD), sputtering, chemical vapor deposition (CVD), radio frequency (r.f) / microwave plasma CVD and others are utilized. The features of a-C films made with diverse processes and precursor materials are summarized in **Table 2.1.**

Table 2.1: Properties of various forms of carbon

	Density ($gmcm^{-3}$)	Hardness G pa	% sp^3	at % H	Gap (eV)	Ref.
Diamond	3.515	100	100		5.5	14
Graphite	2.267		0		-0.04	15
C_{60}			0	0	1.8	16
Glassy C	1.3-1.55	2-3	0		0.01	17
a-C, evap	1.9-2.0	2-5	1		0.4-0.7	18
a-C, MSIB	3.0	30-130	90-15	9	0.5-1.5	19
Pd a:H Hard	1.6-2.2	10-20	30-60	10-40	0.8-1.7	20
PD a-C:H, Soft	0.9-1.6	<5	50-80	40-65	1.6-4	20
Polyethylene	0.92	0.01	100	67	6	21

The study discovered that semiconducting carbon sheets can be intrinsic or extrinsic semiconductors, depending on whether they are doped during or after growth. Carbon-based heterostructures have already been shown in electrical devices such as metal insulator semiconductor (MIS) diodes, scottky diodes, metal insulator semiconductor field effect transistor, hetero junction diodes, thin film transistor (TFT), and silicon solar cells.

The precursor and the carbon film deposition technique are the two most important elements in defining the film's optical and electrical characteristics. As a consequence, these two aspects are carefully examined in the production of a carbon thin film with the required optical and electrical characteristics for application in a range of optoelectronic devices. As a result, research into alternate precursor materials and easy deposition methods has been given top emphasis. Camphor ($C_{10}H_{16}O$) was discovered

as an alternate precursor material in this study because it has some advantages over graphite.

Using camphoric carbon produced from camphor, a natural source, Mominuzaman et al. effectively deposited carbon thin layer using simple ion beam sputtering (IBS) [9]. They also looked at various opto-electrical characteristics and how annealing affected them, taking into account the semiconductive nature of the films and the electrical conduction process. They discovered that carbon thin films made by ion beam sputtering of a camphoric carbon target without the use of an H_2 gas precursor showed optoelectronic properties that were similar to hydrogenated a-C films. The optical absorption coefficient of a deposited layer is 104-105 cm-1, with an optical gap of 0.5 eV.

The optical and electrical characteristics of these films are nearly consistent when annealed up to 4000C, but they vary substantially when annealed above that temperature. At normal temperature, A deposited layer's conductivity is found to be on the order of 10-1 (ohm-cm)-1, but after annealing to 8000C, it becomes graphitic and rises to the order of 101 (ohm-cm)-1.

Mominuzzaman et al., inspired by the previous findings, tried and succeeded in employing camphor as a precursor material in deposition methods other than IBS [10]. Camphor was used as a precursor for the first time in the pulsed laser deposition (PLD) process. They were also successful in producing phosphorus (P) integrated camphoric carbon (CC) films in addition to un-doped CC films. The opto-electrical characteristics of these films, as well as their change due to phosphorus incorporation, were investigated [11]. The optical gap of CC film that hasn't been doped is expected to be around 0.85 eV, and it is essentially stable for films made with up to 5% P targets. Films placed onto a target containing 7% P, on the other hand, shrink the gap to 0.75 eV. The sp^2 fraction has grown due to the decrease in optical gap. The un-doped CC films have a resistivity of around 2x-104 ohm-cm, which increases to 3.7x104 ohm-cm when deposited from a 1 percent P-containing target. The resistivity of films deposited from a target with a larger percentage of P, on the other hand, drops sharply at first and then gradually. They proposed that camphor and other precursors, Based on their

discoveries of camphor carbon films, they may be good starting materials for semiconducting carbon films for electronics applications.

2.4 Basic Knowledge of Thin Film

A thin film is a liquid or solid in which one of its linear dimensions is smaller than the other that is much less than the other two. Typically, thin films are divided (arbitrarily) into the following categories:

Films with a thickness more than one micrometre (D: film thickness),

Films that are very thin (D1 micron);

Rather than unsupported films, this thesis investigates the systems of a (solid) film on a (solid) substrate (backed films) (foils). They (solid substrate) refer to a film-growth technique in which an atomic or molecular flow is maintained on the substrate's surface before film growth begins. Physical processes like as evaporation from a source and sputtering from a target, followed by condensation onto the substrate, will be used to form films, as will chemical interactions of a gas or liquid with the substrate surface.

2.5 The History of Thin Film Technology

R. Boyle, R. Hooke and 1 Newton discovered interference colors of a thin liquid coating on a liquid surface in 1650 A. D. (oil on water). M. Faraday found film formation during glow discharge in 1850 A.D, while W. Grove observed current evaporation of metallic wires the following year.

Solid films made by the first two processes were quickly recognized for their technical value as anticorrosive films or mirror films, whereas those made by the third way lacked repeatability for a long period. Only since the advancements in vacuum equipment for film preparation and analysis (electron microscopy, LEED and other surface analytical techniques) have reproducible and useful films become more easily available. Film production for optical, electrical, mechanical, and protective purposes has seen a rapid increase since 1950. Thin film methods were first used in semiconductor circuits in 1965 and they have two primary advantages: mass manufacturing using printing techniques and downsizing via integration (integration density: elements / mm^2).

2.6 Main Fields of Application

Computer electronics, commercial electronics, medical electronics, space technologies, and energy are all discussed (solar cells).

Metal and dielectric films have optical applications:

* Filters
* Reflection coatings
* Semiconductor optical waveguide for optoelectronic communications Infrared sensors and thin-film laser diodes

For memory and logical devices, magnetic and super conducting films are used. Film formation processes are of basic scientific interest in order to gain insight into the factors that lead to specific structure properties: Regarding the microstructure and macrostructure of amorphous, polycrystalline, single crystal films (microstructure) and island, labyrinth, continuous films (macrostructure) (the mobility of atoms in the films enable relaxation and hereto diffusion).

2.7 Thin Film Deposition Methods

2.7.1 Ion Beam Method

Diamond-like carbon has been created using a number of deposition processes. The growing film is bombarded with medium-energy ions (20-500 V) in each approach, which appears to increase sp^3 bonding [12]-[14]. The various techniques and their growth rates are summarized in **Table 2.2.**

Sputtering carbon sectrodes in an Ar environment in a magnetically controlled plasma was Aisenberg's first ion beam apparatus [15]. The ions are extracted and directed toward the substrate by a bias voltage. When the ions are created from a hydrocarbon source gas, higher growth rates are conceivable.Both a-C and diamond micro crystallites may have been present in the resultant films. Vora and Moravec validated the findings [16],while Motri and Namba looked into the effect of deposition circumstances on film characteristics [16], [17]. **Fig. 2.8** depicts a popular ion source created by Kaufmann [18]. Plasma is formed in this source by combining electrons from a thermion cathode with an axial magnetic field. In a source gas like methane, this results in high ionization rates. A bias electrode extracts positive ions from the source

and directs them to a substrate. Using a cascade source increases the rate of deposition even more.

During the pumping process, The plasma expands supersonically into a high vacuum towards the substrate, resulting in a highly ionized hot methane and Ar plasma.
The plasma gets ionized to a high degree as a result of this expansion.

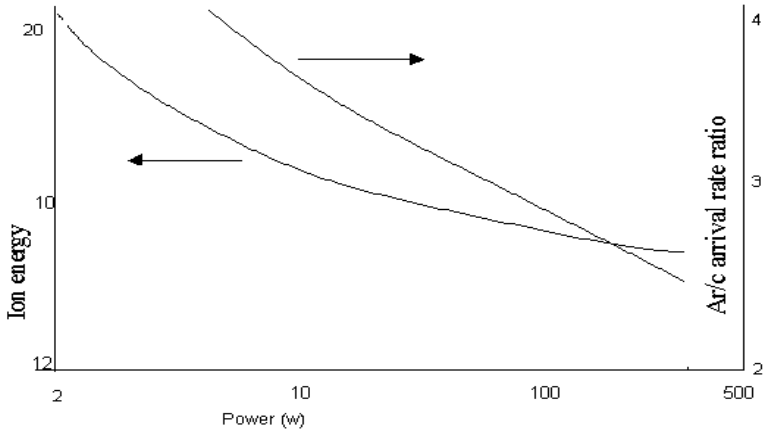

Fig. 2.8 For magnetron sputtering, the arrival rates of Ar+ and C atoms vary with sputtering strength [43]

If the ion beam is passed via a magnetic mass analyser for c/m selection, a single ion species can be deposited. Only a pure beam of C+ (or C-) ions reaches the substrate after the analyzer filters out neutrals, cluster species, graphitic fragments, and contaminants.

The produced material is fully amorphous, with the largest sp^3 bonding percentage of any deposition technique now available, according to structural investigations reported subsequently. The deposition rates for employing carbon as an ion source can be maximized using this strategy in **Fig. 2.8**. The typical rate is now 400 A/min. For stability, they are magnetically confined. The key practical issue with this technology is that the films have a high compressive stress. As a result, their adhesion is limited, as is the maximum stable film thickness.

Table 2.2: Carbon-like Diamond deposition methods.

	Precursor	Typical Growth Rate, A/sec.
Ion beam	Methane	2
Ion beam	Graphite	1.3
PD	Benzene	15
PD	Methane	1
Ion plating	Benzene	10
Magnetron Sputtering	Graphite	3
Cascade are	Methane/Ar	300
Laser Plasma	Graphite	<3
Ar beam sputtering	Graphite	3
Mass selected ion beam	Graphite	0.1-6

2.7.2 Sputtering

To make hard carbons, a variety of sputtering techniques can be used. Typically, a 1 kV beam is used. Ion beam sputtering uses Ar ions to bombard a graphite target [19],[20]. To enhance the yield, a 30-450 degree angle of incidence is used. The carbon sprayed onto an adjacent substrate condenses. To attack the growing layer with ions, It's possible that a second Ar ion beam will be focused on the substrate. The low sputtering rate of graphite is linked to poor ion beam sputtering deposition rates.

Faster deposition rates are possible using magnetron sputtering. As demonstrated in the figure, Ar plasma is employed to both sputter from the target and bombard the growing film in **Fig. 2.8**. Growth rates are typically 3 A/sec and change linearly with rf power [21]. Ion energies are in the 20 eV range, and they gradually drop as power or gas pressure is raised. The substrate is blasted with a combination of Ar and carbon ions and atoms. As the sputtering power is reduced, the ion/atom ratio in the beam rises, according to Savvides [22], because the ion yield reduces more slowly than the neutral atom flow in **Fig. 2.8**.

This is the inverse relationship to plasma deposition, where ion bombardment increases as plasma strength increases. You can individually apply a dc bias to the substrate to boost the mean ion energy. Sputtering methods offer improved process control and the

capacity to scale up for mass production. The most durable films appear to be made with low power and low gas pressure, resulting in slower deposition speeds.

2.7.3 Plasma Deposition

Plasma breakdown of a hydrocarbon source gas onto negatively self-biased substrates is the most common deposition method. Holland and Ojha were the first to synthesize a-ST using plasma deposition (PD) or simply plasma-assisted chemical vapour deposition (PACVD) [23]. For a-C: H, self-biasing is preferred over dc biasing since the films are insulating. In this approach, The substrate electrode is capacitively coupled to the rf power, and the counter electrode is either a second electrode or the deposition chamber's grounded walls in **Fig. 2.9.**

As a result, the electrode diameters differ significantly. If the rf frequency is higher than the ion plasma frequency, which is in the range of 2-5 MHz, the electrons can follow the rf voltage. A negative dc is produced by the substantial difference in electrode size as well as electron and ion mobility. The energized electrode becomes cathode due to self-bias. Throughout each rf cycle, the compensating electron current runs in brief bursts, making the ion current mostly dc in **Fig. 2.9.**

The discharge now has a glow area, where ions are created by collisions with electrons, and an ion-sheath, where the ions are driven to reach the cathode. A resistance for the plasma glow in series with a capacitance for the sheath is the corresponding electrical circuit for the plasma. Across the sheath, the dc bias is virtually eliminated in **Fig. 2.10.**

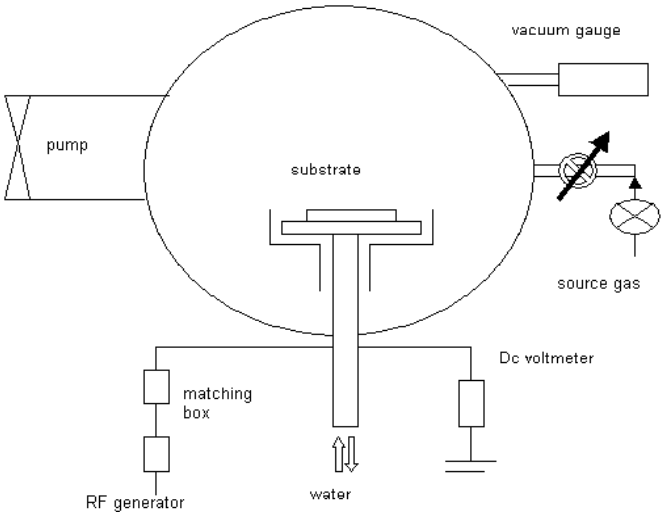

Fig. 2.9 The substrate is linked to the powered electrode in this schematic of a capacitively coupled Rf plasma deposition device [43]

The bias voltage, - Vb varies with rf. power W and operating pressure P as

Vb = k (W/P) ½…..…. [2.1]

Variables such as electrode areas influence the value of k. This is the expected link for ohmic plasma and a P-1/2 sheath thickness, according to Catherine and Couderc. At low pressures and without collisions, the ion energy E1 is determined by V and the ion mean free path in the sheath.

E1 = eVb……..... [2.2]

At higher, average operating pressures, there is a range of ion energies with a mean value of

E1 = k/Vt/p1/2 ..... [2.3]

For a typical pressure of 3 Pa, E1 = 0.6Vb For Ar discharges, Koidl et al. examined the ion energy spectrum [24].

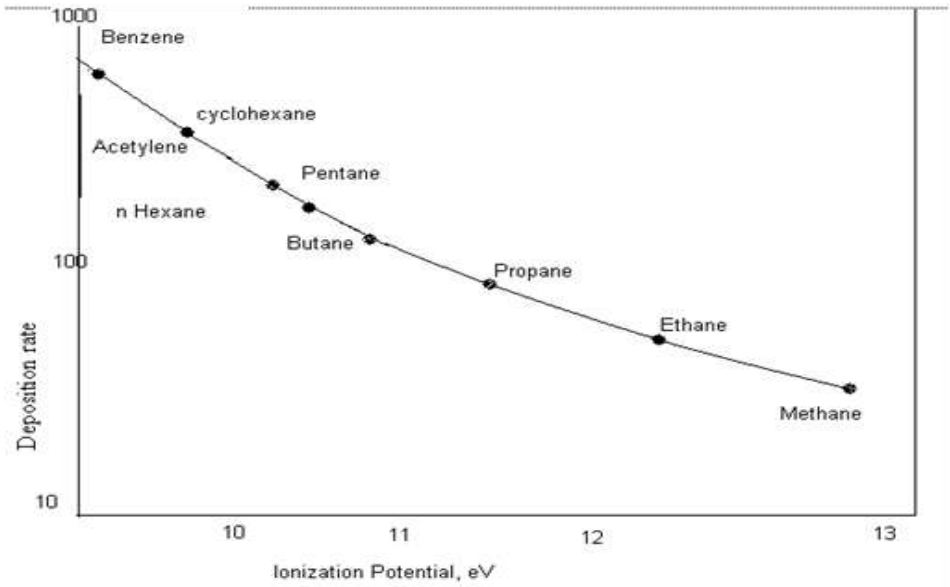

Fig. 2.10 Plasma deposition rates versus ionization potential of precursor gas, for a gas pressure of 3 Pa and a self-bias voltage of 400v [43]

As illustrated in **Fig. 2.10**, The deposition rate is influenced by the source gas's ionization potential and molecular weight, with low ionization potentials and large molecular weights resulting in fast growth rates. It has been established that the deposition rate v for a certain gas varies with bias voltage and gas pressure as follows:

$v = k V_b P$ ……..... [2.4]

When the incoming ions begin to sputter the film at biases greater than 1.2-1.5 kV, the deposition rate can saturate or fall. Koidl et al. discuss a range of different source gases (Benzene, acetylene, and methane) [24].

The problem scaling up to bigger systems using PD derives from the fact that bias voltage and as a result, electrode areas have a greater influence on film characteristics than process factors such as RF power and gas pressure. The characteristics of PD a-C: H are influenced by the ion energies. The source gas is only weakly dissociated at low ion energies, resulting in a highly hydrogenated or polymeric form of a-C:H. Plasma polymerization is comparable to this method. Another common method for making a-Si:H and polycrystalline diamonds is plasma deposition, however the requirements differ dramatically in each instance, as indicated in **Table 2.3**. To create hard a-C: H during deposition, To receive positive ions, you'll need a cathodic substrate, a high RI:

power (for a high bias voltage), low gas pressure (for high ionization), and low substrate temperatures (to minimize self-annealing).

Table 2.3: Plasma deposition of a-C: H electronic grade a-Si: H and polycrystalline diamond under certain conditions.

	a-C:H	a-Si:H	Diamond
RF power density, W/cm^2	1	0.01	10
Gas pressure, Pa	3	10	3
Substrate electrode	Cathode	Anode	
T_0, ^0C	25	2.50	800
Dilution			H_2/CH_4=100

Electronic grade a-Si:H is deposited from saline plasmas under circumstances that limit defect state concentration due to dangling Si bonds. Enough hydrogen must be conserved to passivate the dangling bonds, but not so much that polymeric SiH_2 groups become prevalent. To achieve optimal self-annealing, gentle circumstances of low RF power density, moderate gas pressure, anodic substrate (to decrease ion bombardment) and a substrate temperature of around 2500C are required. The utilization of hydrogen-diluted source gases, a high power density and a higher substrate temperature all help diamond formation. As a result of these conditions, atomic hydrogen is produced, which inhibits graphite and a-C deposition via a variety of mechanisms, including favoured etching. For example, Ion plating is a hybrid deposition process in which the plasma is created by RF plasma and the ions are then pushed by a separate field from a grid electrode to the substrate [25].

Microwave discharges, in particular when operated at the electron cyclotron resonance, can create plasmas that are more intensely ionized. This method produces significant ion densities even at low gas pressures. Due to the lack of electrodes and the capacity to modify the shape and position of the plasma, this technology is theoretically interesting. Both ionization and ion energy may be adjusted using a microwave ion source with an rf self-biasing accelerator.

2.7.4 Laser Methods

How laser ablation of graphite can form carbon ion plasma shows in **Fig. 2.11**.The generated plasma is most likely similar to that produced by a catholic are. When the

laser power density exceeds a threshold amount, the resulting a-C has a diamond-like appearance.When the laser power density exceeds a threshold, the resulting a-C takes on a diamond-like appearance.

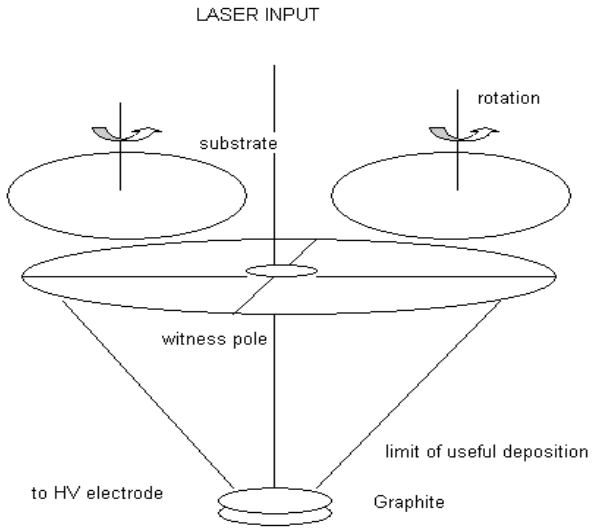

Fig. 2.11 Laser-plasma deposition apparatus [43]

2.7.5 Chemical Methods

2.7.5.1 Electroplating

Only metals and alloys may be deposited on electrically conductive substrates using this approach. The electrolyte contains positive ions from the film substance. The mass of the deposit is determined by the number of ions discharged at the cathode and hence by Faraday's law.

$m/A = jt M\alpha/n F$ ..... [2.5]

Where m/A stands for mass per area, j stands for current density time, M stands for molecular weight, n stands for valence, F stands for 96490 As/g equivalent, and 1-0.5 stands for current efficiency. Al, Ag, Au, Cd, Cu, Cr, Fe, Ni, Pb, Pt, Rh, Sn, and Zn are among the 70 metallic elements that may be electrodeposited, although only 14 of them are routinely deposited: Al, Ag, Au, Cd, Cu, Cr, Fe, Ni, Pb, Pt, Rh, Sn, and Zn.

Physicists are interested in the underlying process of discharge and film production: Ions (of both types) are forced towards the oppositely charged electrode, where they form a double layer that protects the bulk electrolyte from the main component of the electric field. The voltage lowers in the double layer (about 30nm thick), resulting in

high field strengths (107 V cm-1). Before being absorbed into the films, positive ions in an aqueous solution go through a number of processes: Dehydration, discharges, surface diffusion, nucleation, and crystallization are all terms used to describe the processes of dehydration, discharges, and surface diffusion.

Table 2.4: Summary of film properties prepared by ion beam and sputter deposition.

Deposition Conditions				Properties of hard a-C films			
Condensation of carbons (ion beam deposition)	Source of carbon	Ion energy (eV)	Density (g/em)	Electrical resistivity (* cm)	Optical proprieties	Hardness (kg/mm^2) (HN or HK)	Chemical meartness
	Carbon in rf plasma	40-100		~ 10^{10}	Refractive index. F=2.0	> Glass	Resist HF for 40 hi 10-20 yr archive lifetime
	Carbon in nrc^h	50-100		>10^{12}	n~2		
	Carbon in de plasma	50-100		Dielectric constant ~6 (diamond = 5.7)	n = 2.3 nt λ = 5 wn	185 QHK (diamond 7000 HK)	
Sputtering deposition	Carbon target in rf. plasma	Rf power = 2.25 and 75W	10^{-2}-10^3	Optical gap E_0~08cV			
	Carbon Sputtered by Ar beam	1-20	2.1-2.2	>10^{11}	Reflectance 0.2 Absorplance 0.7 Absorption coefficient α=6.7x10^4 cm^{-1} transmittance 0.1		
	Dc Magnetron Sputtering of a graphite target	Sputtering power density W cm^{-2})		(At 300K)	n (at λ = 1μm)	E_n (eV)	HN
		0.25	2.1-2.2	2.5x10^4	2.4	0.74	2400
		2.5	1.9	1.0	2.73	0.50	2095
		25	1.6	0.2	2.95	0.04	740

While depositioning alloys, different electrochemical potentials affecting the ratio of discharged ions of the components at a given voltage must be addressed. Chemical complexing of ions can be used to alter the particular discharge processes. At a current density of 1 Acm-1, the high growth rates D=dD/dt=1s-1 are a unique attribute of electrode placement.

2.7.5.2 Spin coating:

Spin coating, also known as spin casting, is the method of depositing a liquid precursor, such as a sol-gel precursor, onto a smooth, flat substrate and centrifugally dispersing the solution throughout the substrate. The spinning speed of the solution and the viscosity of the solution determine the final thickness of the deposited layer. Depositions can be repeated as many times as necessary to increase the thickness of the films. To crystallize the amorphous spin coated film, thermal treatment is commonly utilized. After crystallization on single crystal substrates, such crystalline films might have particular preferred orientations.

2.7.5.3 Electro less Plating (Chemical-Reduction Plating)

Some electrochemical reactions, such as mirror silvering by $AgNO_3$ solutions containing formaldehyde or sugar as a mild reducing agent can take place in the absence of an external field. This reaction occurs on any submerged surface in the bath. On rare occasions, the reaction happens only on certain surfaces:

NiC1+ sodium hypophosphite $\rightarrow$ Ni deposit only on Ni, CO, Fe and Al surfaces .....……..... [2.6]

2.7.5.4 Chemical Vapour Deposition (CVD)

Such approaches that rely on a gas transport response are crucial in the production of semiconductor devices [26]. Typically, the film material is a component of a volatile molecule that decomposes in a heterogeneous reaction at the substrate. Elevated temperatures are frequently required to permit single crystal film growth on a suitable substrate, which is virtually always iso-epitaxial Si on single crystal growth.

2.7.5.5 Anodization

The breakdown of H2O at the anode of an aqueous electrolytic system produces an extremely reactive state because atomic oxygen is the reacting partner. The reactions are:

a: $M + nH_2O \rightarrow MO_n + 2nH^+ + 2ne$.....……..... [2.7]

c: $2ne + 2nH_2O \rightarrow nH_2 + 2nOH$ .....……..... [2.8]

2.7.5.6 Thermal Growth

When a reactive material surface, such as Pb or Al, is exposed to the environment at ambient temperature, an oxide layer forms. The process of oxidizing semiconductors in water vapor at high temperatures is particularly essential in semiconductor technology (about 10000C). SiO_2 has strong insulating and protective characteristics as a result of this process. If the reactive gas is NH_3, Ni-tridization is also conceivable. When a reactive plasma is formed and the ions are directed towards the substrate, the temperature can be decreased in general. A parabola is the shape of the growth curve.

Summary of the ways of preparing thin are shown in **Table 2.5.**

Table 2.5: Summary of ways of preparing thin films.

Method	Deposition Rate As^{-1}	Rate Control	Type*	Advantages	Limitations
Electro-Plating	10^2-104	Current density	M	Simple apparatus	Metallic Substrate
Chemical Reduction	10	Solution temp, p^{11}	M	Simple apparatus	Limited number of materials
Vapor	$1\text{-}10^3$	Pressure, temperature	M, S, I	Single crystal, Clean films	High substrate temperature, low pressure
Anodization	10	Current density	1	Simple apparatus, Thin amorphous Films	Metallic substrate limited no. of metals, limited thickness
Thermal	1	Pressure, Temp	M, S, I	Simple apparatus	Metallic substrate, Limited thickness Limited no. of Metals
Evaporation	10-103	Source Temp.	M, S, I	Large range of materials and substrates	Vacuum apparatus, Some materials Decompose on heating
Sputtering	10	Current potential	M, S, I	High adhesion, very large range of materials	Suitable targets, Vacuum apparatus

2.7.6 Un-doped Camphoric Carbon (CC) Films

Carbon thin films have a number of unique characteristics and these properties may be changed in a wide range of ways, attracting an increasing number of researchers to the subject of carbon thin film research [27]. On the other hand, these films' characteristics are heavily influenced by the precursor material and deposition technique. The inclusion of hydrogen affects the properties of a-C thin films and adds a significant number of sp^3 sites, causing the band gap to expand. Since a long time, graphite has been widely employed as a target material. The structure of graphite is made up entirely of sp^2-hybridized carbon is shown in **Fig. 2.12**. The sp^3 bond promotes the creation of

diamond-like carbon (DLC) films, which are superior to thin films. In the case of graphite, extra hydrogen must be supplied when a film is hydrogenated to modify its characteristics, whereas the camphor molecule already has sufficient of hydrogen in its structure. Camphor ($C_{10}H_{16}O$) has been proposed as an alternative precursor material for the deposition of carbon thin films due to its benefits over graphite. In the following subsections of **table 2.5**, the experimental specifics of the deposition of thin films from camphor targets, as well as various features of these films, will be examined.

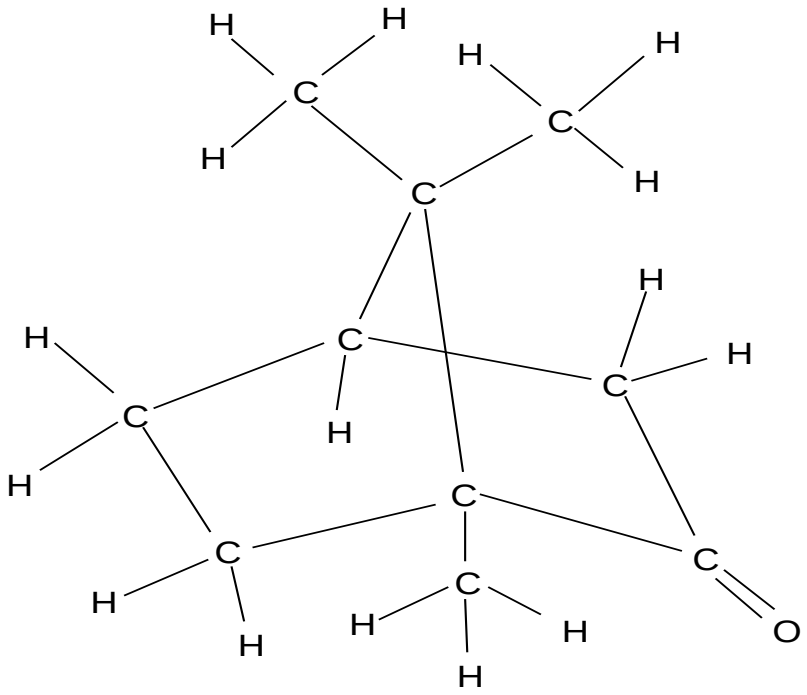

Fig 2.12 Chemical structure of camphor [42]

Chapter 3

METHODOLOGY

3.1 Carbon Thin Film Deposition by Electroplating

Carbon thin films have received a lot of attention recently due to their potential applications as hard, wear-resistant films and optical coatings. Carbon thin films have been deposited using vapor deposition techniques such as chemical vapor deposition, pulsed-laser deposition, and ion-beam sputtering.

According to experimental data, Electroplating technologies can deposit most compounds that can be deposited in the vapor phase in the liquid phase. For electroplating, we employed a methanol solution in our lab. Methanol was chosen because it has a higher polarizability and conductivity than ethanol and has a structure that is even closer to diamond than ethanol.

Carbon films' optical and electrical characteristics are mostly determined by the precursors and deposition technique. Camphor ($C_{10}H_{16}O$) was found as an alternative precursor material in this study due to various advantages it has over graphite. Camphor has both sp^2 and sp^3 hybridized carbon, while graphite contains exclusively sp^3 hybridized carbon. Furthermore, camphor molecules with sp^3-hybridized bonds enhance the deposition of carbon films, particularly diamond-like carbon (DLC) films. Naturally, we're intrigued by the prospect of utilizing camphor as a deposition precursor. In this article, the electrolysis technique is used to try film deposition. Methanol CH_3OH and various camphor concentrations (1% ,2%, 3%, 4%, 5%, 6%, 7%, and 8%) in methanol are used as electrolytes.

Fullerenes, which were long considered exotic, are now frequently produced and employed in study thanks to recent developments in the science of crystalline carbon. Among them are bucky balls (C_{60}), carbon nanofibers, single-walled carbon nanotubes (SWCNT), multi-walled carbon nanotubes (MWCNT) and other carbon nanomaterials. Carbon nanotubes with their superior mechanical and electrical properties, are a promising new useful material for next-generation electronics. Nonetheless, a commercial application faces a few challenges. Controlling carriers in carbon nanotubes is crucial before they can be used in transistors in industry [28]. The optical

characteristics of carbon nanotubes are used in materials research for absorption, photoluminescence, and Raman spectroscopy. The technique of electrolysis is used to try film deposition in this article. Electrolytes include methanol (CH_3OH) and SWCNT, MWCNT, Fullerene, Graphite (0.1 percent) in methanol. A schematic representation of the system is shown in **Fig. 3.1.**

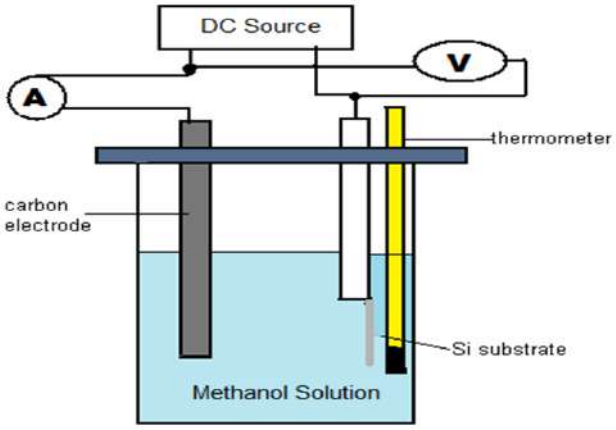

Fig. 3.1 Schematic Diagram of Electro Deposition

3.2 Experimental Details of Electroplating

An experimental layout in Electrical Circuit Lab, Dept. of EEE, IIUC is shown in **Fig. 3.2.** In this electroplating procedure copper, aluminium, zinc or silicon substrates measuring 3.2x1.5x0.1 cm3 were put on the negative electrode. Pure water is used to clean the substrates in order, CH_3COCH_3 solution, CNT solution and CH_3OH layout solution. The distance between the positive electrode and the substrate was fixed to 1.5 cm. From 0 to 2500 V, the potential delivered to the substrate might be adjusted.

Fig. 3.2 Experimental Layout in Electrical Circuit Lab, Dept. of EEE, IIUC

The device is equipped with a thermometer that monitors the temperature of the fluid as it is deposited. Methanol electrolysis was used to deposit carbon thin films on aluminum (Al), copper (Cu), zinc (Zn), and silicon (Si) substrates. Carbon nanomaterial (0.1%) mixed in methanol. The effect of methanol integration with camphor (C_{10} $H_{16}O$) and CNT material (SWCNT, MWCNT, Graphite, Fullerene), a natural source is examined. With varied percentages of camphor content, there was a noticeable difference in the variance of current density as a function of applied potential. Thin films with varied percentages of camphor were deposited on Al, Cu, and Si substrates and compared. The current density appears to change depending on the substrate.

3.3 Carbon Thin Film Deposition by Spin Coating

Coating (casting) a solvent-based solution of the desired substance (an "ink") while the substrate is spinning, a thin layer is placed evenly across the surface of the substrate. Alternatively, a liquid solution is deposited onto a spinning substrate to form a thin layer of solid material, such as a polymer.

The centripetal force combined with the surface tension of the solution drives the liquid coating into an even covering when the substrate is spun at a high speed (typically more than 10 revolutions per second = 600 rpm). During this time, the solvent evaporates, leaving the desired chemical in an even layer on the substrate [29]. A schematic diagram of the Spin Coater is shown in **Fig. 3.2.**

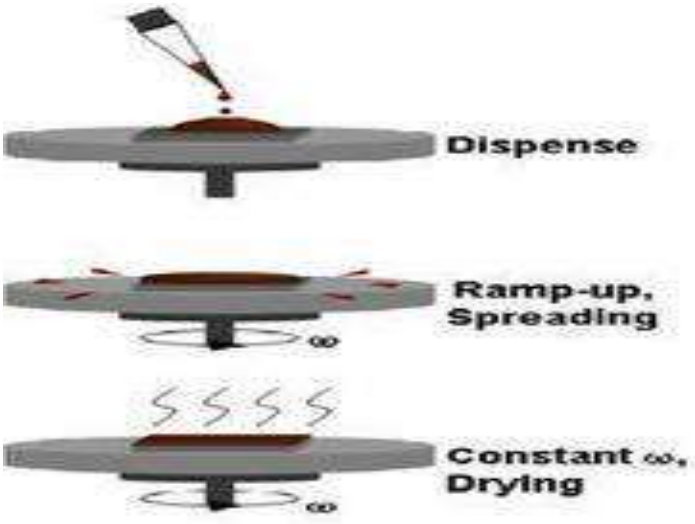

Fig. 3.3 Schematic Diagram of Spin Coater

3.4 Experimental Details of Spin Coating

The vacuum spin coater VTC 100 at BCSIR, Dhaka, was used to conduct the spin coating is shown in **Fig. 3.4**. Prior to deposition, the substrates were cleaned with electronic grade acetone (CH_3COCH_3) and methanol (CH_3OH) for 5 minutes at 55 degree celcius. To make the electrolytes, MWCNT was combined with various amounts (0.1 percent and 0.2 percent) in methanol solvent. For 60 seconds, the substrate with the electrolytes was spun at 500 rpm and then at 3000 rpm.

Fig. 3.4 VTC 100 Vacuum spin Coater in BCSIR, Dhaka

3.5 SEM and EDS analysis

3.5.1 SEM analysis

SEM (Scanning Electron Microscopy) is one of the most extensively used techniques for analyzing nanomaterials and nanostructures. The SEM has a resolution of a few nanometers and can work at magnifications ranging from -10,000 to over 300,000. It enables non-destructive testing of a wide range of materials. A source of electrons is focussed into a beam with a very small spot size that is swept over the surface of the material by deflection coils in a standard SEM. A multitude of interactions occur as the electrons impact and penetrate the surface, resulting in the emission of electrons and photons from the sample, and SEM images are created by collecting the released

electrons on a cathode ray tube (CRT). A sample of SEM picture is shown be in **Fig. 3.5**.

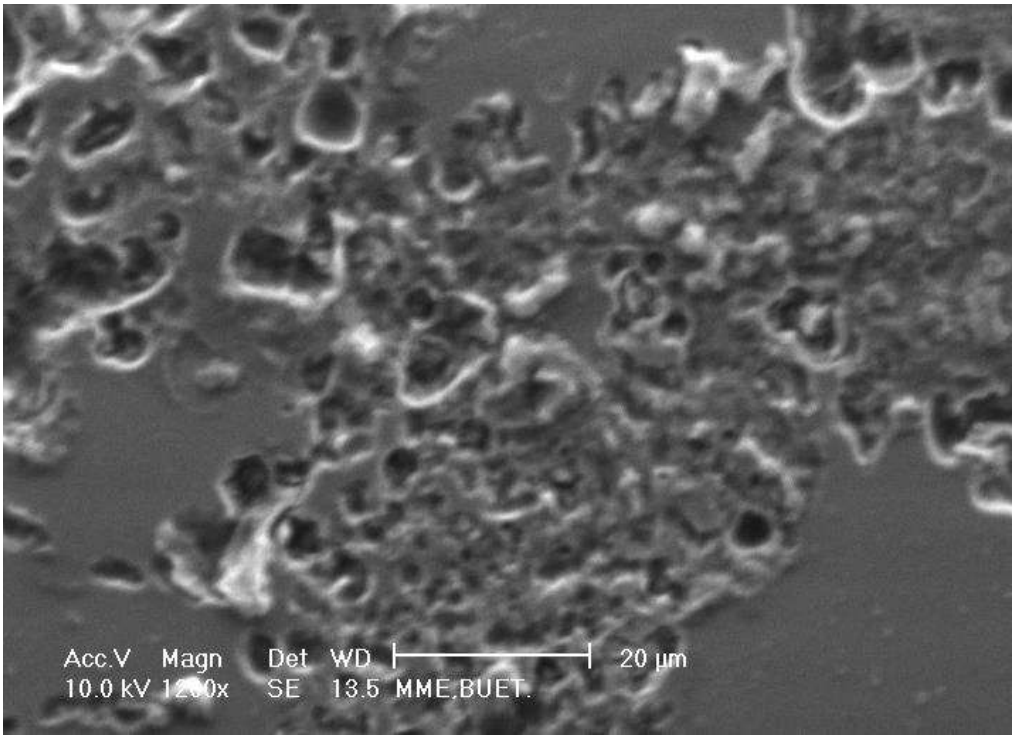

Fig. 3.5 SEM micrograph of the film deposited in 2% camphor in methanol solution on Si substrate [30].

3.5.2 EDS analysis

EDS (energy dispersive X-ray spectroscopy) is a technique for analyzing the elements (elemental composition) present in a material. EDS is a method that is widely used alongside SEM and TEM to determine the relationship between composition, microstructure, and elemental spectra.

3.5.3 Experimental details

An electron beam is tightly focussed onto the specimen's surface, and X-rays emitted from the surface are evaluated spectrally or energetically by a crystal spectrometer or proportion counter in this procedure. A dispersive spectrometer is a device that employs an analyzing crystal to extract certain wavelengths from a spectrum in order to identify and quantify elements is used to study the emitted X-ray. An Electron Probe Micro Analyzer is shown in **Fig 3.6.**

The amount of electrons absorbed, the number of electrons back scattered without energy loss since they do not contribute to X-ray excitation, and other variables all have an influence on the probe's X-ray excitation.

Samples are polished flat (to ensure that emergent X-rays from all points on the surface have the same path length) and possibly etched to bring out surface characteristics for investigation.

Specimen Stage

X-ray Analyzer

X-ray Method

Electron probe

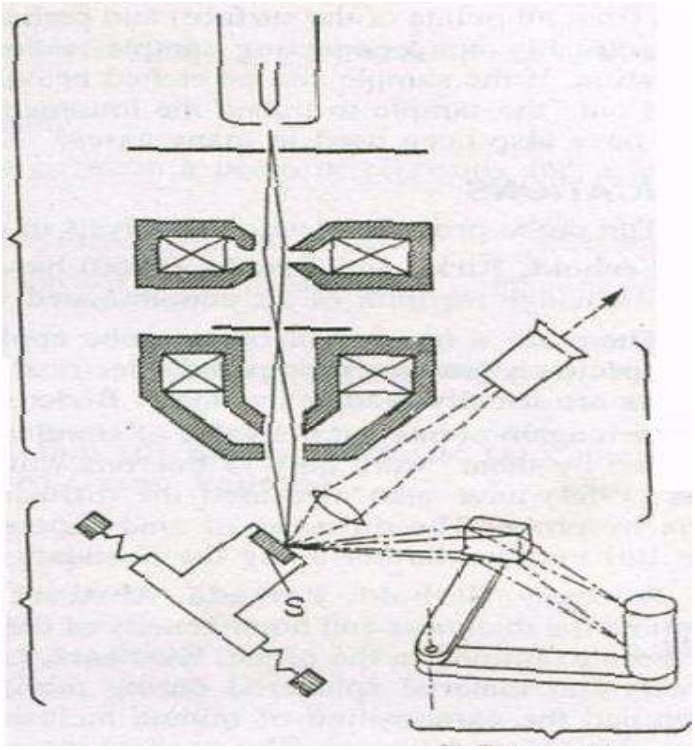

Fig 3.6 Electron Probe Micro Analyzer [34]

3.5.4 Film Composition

For detecting SEM and EDS on Al, Cu, Zn and Si substrates, a JEOL JSM -7600F field emission scanning electron microscope was used which is in GCE lab, BUET, Dhaka, as illustrated in **Fig. 3.7**.

Fig. 3.7 JEOL JSM-7600F field emission scanning electron microscope in GCE lab, BUET, Dhaka

Chapter 4

RESULTS AND DISCUSSION

4.1 Previous Works Done on Carbon Thin Film Deposition:

Summary of the works done so far on carbon thin film deposition are tabulated in **Table 4.1**

Table 4.1: Summary of the Works Done on Carbon Thin Film Deposition

Deposition Technique	Solution	Substrate	Material	Characterization Techniques
Electro Deposition	Methanol	Al Cu Si	Camphor	• Measurement of P^H • Measurement of Current Density • SEM Analysis • EDS Analysis
Electro Deposition	Methanol	Zn	Camphor	• Measurement of P^H • Measurement of Current Density • SEM Analysis • EDS Analysis
Electro Deposition	Methanol	Si	Fullerene Graphite MWCNT SWCNT	• Measurement of P^H • Measurement of Current Density • SEM Analysis • EDS Analysis
Spin Coating	Methanol	Si	Fullerene Graphite MWCNT SWCNT	• SEM Analysis • EDS Analysis

Here some of the works are done by our supervisor and some of the works are done under his supervision in undergraduate level. Now we are comparing those works. Here two deposition techniques were used which are Electrodeposition and Spin Coating. Methanol was used as solution in all of these experiments.

As substrates Al, Cu, Si and Zn were used. As deposition material Camphor and CNT materials (Fullerene, Graphite, SWCNT and MWCNT) were used. Different characterization techniques were observed like measurement of P^H, measurement of current density SEM analysis and EDS analysis.

4.2 Measurement of P^H

4.2.1 Analyses of the role of camphor in methanol solution by P^H

The P^H of an organic solution is critical in the making of a film. The influence of camphor on deposition rate is explained in **Table 4.2** of P^H as a function of camphor in methanol. The P^H of the solution rises before deposition as the proportion of camphor in methanol rises and gradually lowers after deposition as the proportion of camphor in methanol declines.

The P^H of methanol containing 1% camphor is approximately 2.4 before deposition. With increasing camphor content, the P^H has risen to 4.5 before deposition for methanol with 5% camphor. On the other hand P^H of methanol containing 1% camphor is approximately 8.1 after deposition. With increasing camphor content, the P^H has decreased to 5.3 after deposition for methanol with 5% camphor. The change in P^H before and after deposition reveals that the films are made from a methanol solution containing camphor.

Table 4.2: P^H for several percentage of camphor in methanol solution are measured before and after deposition [34]

Materials	P^H Before Deposition	P^H After Deposition
1% Camphor	2.4	8.1
2% Camphor	3.3	8.0
3% Camphor	3.7	7.5
4% Camphor	3.9	6.3
5% Camphor	4.5	5.3

4.2.2 Analyses of the role of carbon nanomaterials in methanol solution by P^H

The influence of carbon nanomaterials on deposition rate is explained in **Table 4.3** of P^H as a function of carbon nanoparticles in methanol. P^H of the solution is greater in after deposition than before deposition with the increasing percentage of carbon nanomaterials in methanol solution.

Before deposition, the P^H of the solution containing 0.1% mixed fullerene is 5.1 and it rises to 5.8 containing 0.2% mixed fullerene. Then after deposition, the P^H of the solution containing 0.1% mixed fullerene is 6.4 and it rises to 7.1 containing 0.2% mixed fullerene. P^H of the solution remains same with increasing the percentage of MWCNT and SWCNT before deposition in methanol. But after deposition P^H of the solution fell to 4.4 from 4.7 with the increasing percentage of MWCNT and rises to 5.8 from 5.4 with the increasing percentage of SWCNT.

Table 4.3: Before and after deposition, the P^H of various percentages of carbon nanomaterials in methanol solution was determined [33]

Carbon Materials	P^H Before Deposition	P^H After Deposition
0.1% Mixed Fullerene	5.1	6.4
0.2% Mixed Fullerene	5.8	7.1
0.1% MWCNT	2.3	4.7
0.2% MWCNT	2.3	4.4
0.1% SWCNT	2.3	5.4
0.2% SWCNT	2.3	5.8

4.2.3 Findings from Measurement of P^H

- Changes in P^H were observed due to variation of amount of carbonic materials in methanol solution.
- The carbonic materials are influencing the ionic position in the solution.
- Changes in P^H were observed before and after deposition in methanol solution.
- Changes in P^H before and after deposition indicates any chemical changes on the substrates.

4.3 Measurement of current density using camphor in methanol

The substrate current is crucial when making a film from an organic solution. More ionized charge particles are moving from the solution to the electrode at a higher current density, delaying the film's growth. Current densities are calculated for a variety of applied voltages and electrolytes. At a greater current density, more ionized charge particles are flowing from the solution to the electrode.

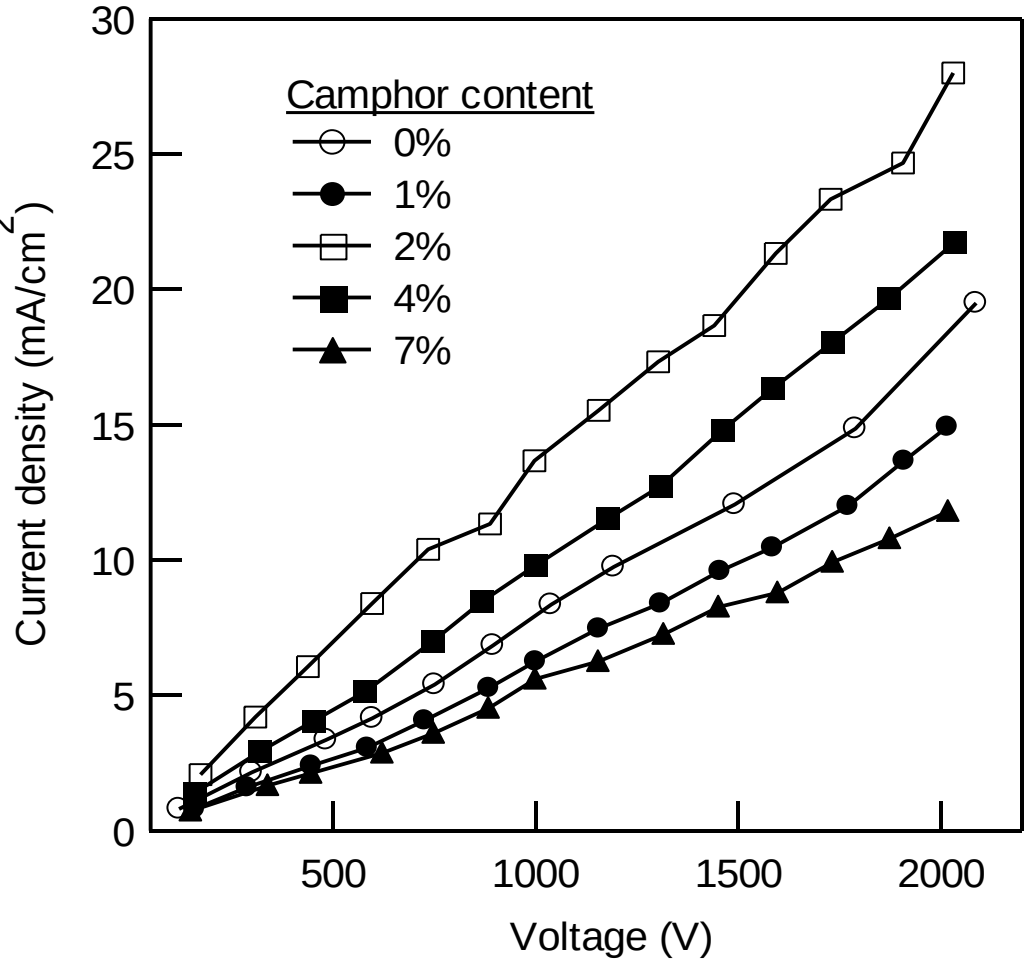

Fig. 4.1 Current density of the Al substrate as a function of applied voltage in relation to methanol with various camphor percentages (0%, 1%, 2%, 4% and 7%) [30]

The amount of camphor to use in a methanol solution to achieve the highest current density was established for Al. Camphor concentrations of 0 percent, 1%, 2%, 4%, and 7% were investigated. The effect of various camphor percentages on current density was examined. On an aluminium substrate, compares current density as a function of applied voltage for increasing concentrations of camphor in methanol solution **Fig. 4.1**. For 0% camphor content, a small current density pattern was obtained (only methanol solution). By adding a small amount of camphor (1%) to the solution, the current density is lowered from that of a pure methanol solution. The current density rose as the camphor content (2%) increased, reaching a maximum value. The existing density has been reduced in order to boost the camphor content further. The current density of methanol containing 4 % camphor was somewhere between 2%

and 0%. The current density reduced even further for 7% camphor content, dropping to a value less than 1% camphor, indicating that the solution was saturated with camphor.

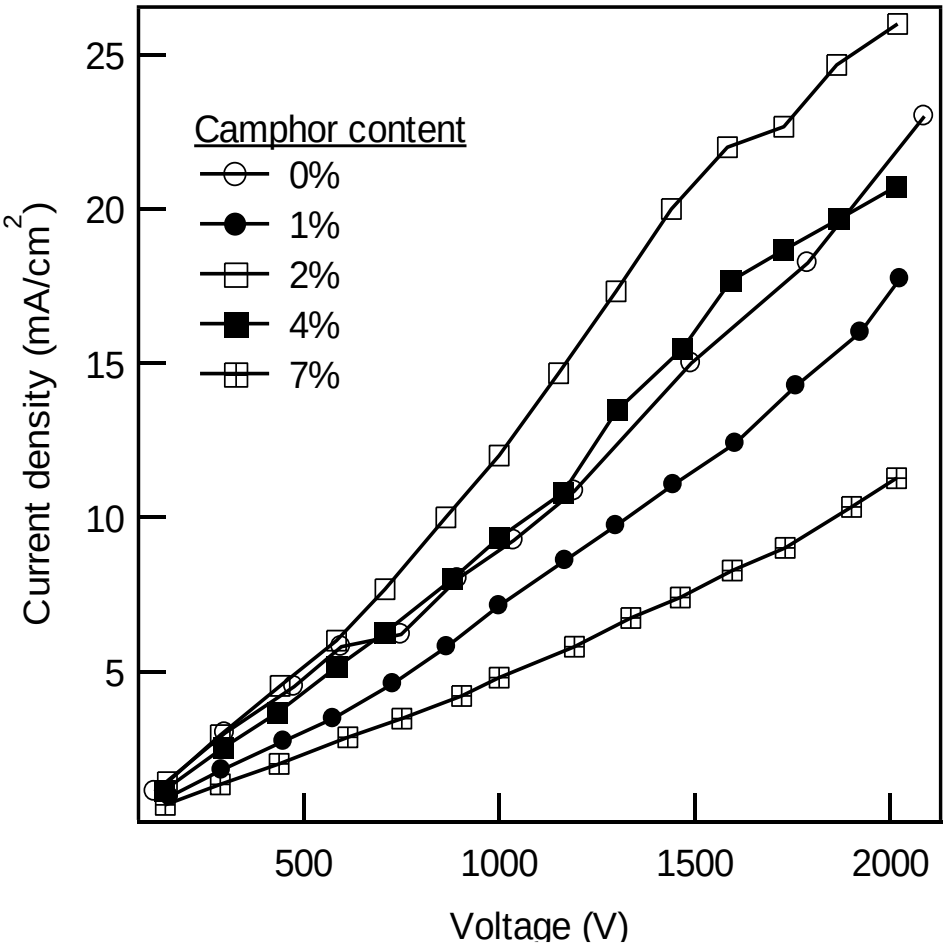

Fig. 4.2 Current density of the Cu substrate in response to methanol with varying camphor percentages (0%, 1%, 2%, 4% and 7%) as a function of applied voltage [30]

The current density as a function of applied voltage is also measured for the Cu substrate. The current density of Cu substrates changes with applied voltage in the same way as the current density of Al substrates varies with applied voltage. The fluctuation of current density with applied voltage for Cu substrates is shown in **Fig. 4.2.** The current density is initially reduced by camphor (1%) and then enhanced by camphor in a methanol solution containing 2% camphor. The current density, on the other hand, decreases as more camphor is added. While the sequential changing pattern of current densities for Al and Cu is similar, the amplitude of current densities for the same circumstance is not.

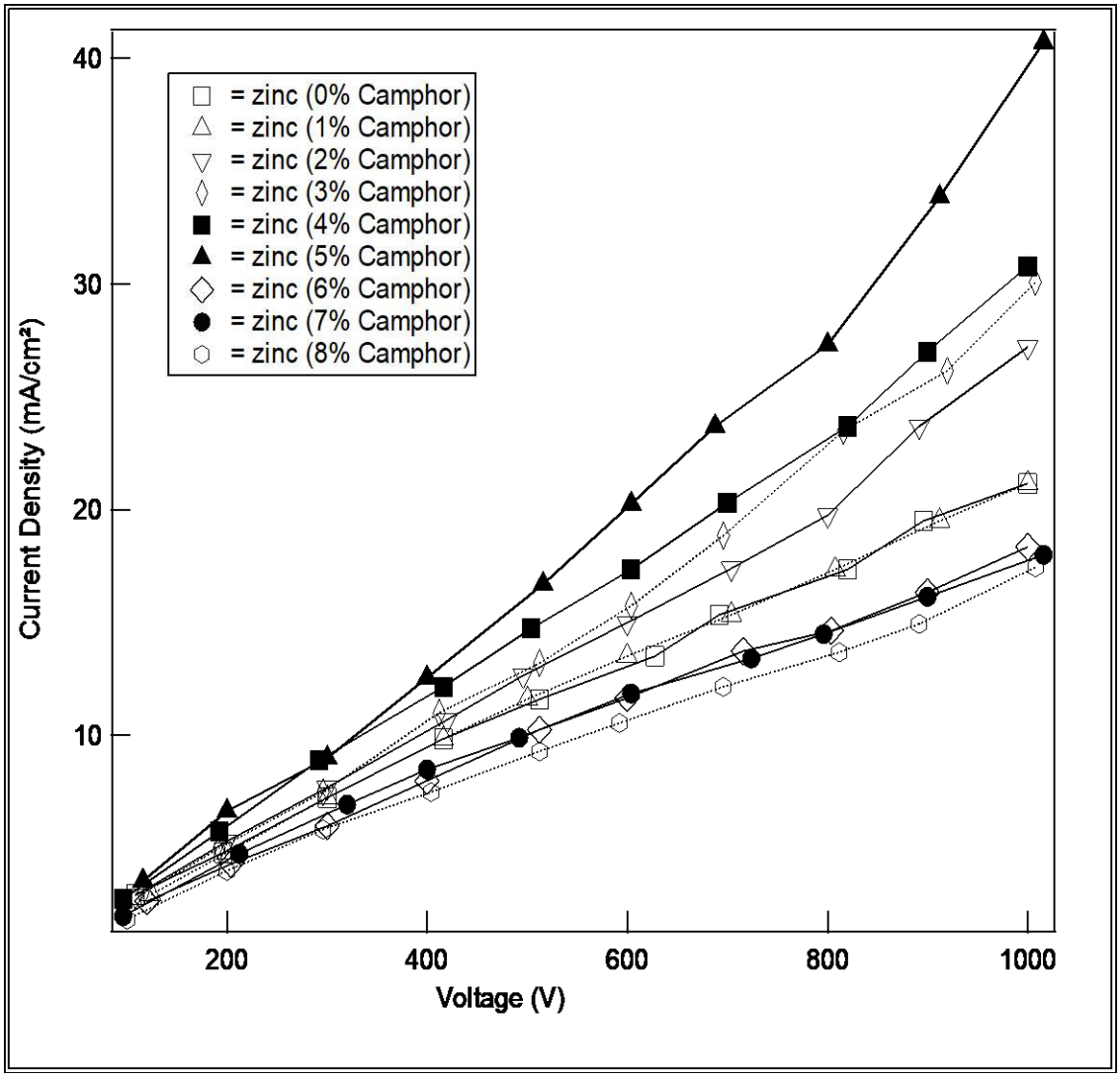

Fig. 4.3 Current density of the Zn substrate as a function of applied voltage in proportion to methanol with different camphor percentages (0,1%, 2%, 3%, 4%, 5%, 6%, 7%, and 8%) [34]

The current density was determined to be highest in the case of Zn substrate for an optimal quantity of camphor in methanol solution. Camphor concentrations 0%,1%, 2%, 3%, 4%, 5%, 6%, 7% and 8% were tested. The effect of different percentages of camphor on current density was investigated. **Fig. 4.3** compares current density as a function of applied voltage for different percentages of camphor in methanol solution for Zn substrate. A modest current density pattern was obtained for 0% camphor content (just methanol solution). The density of the current is enhanced from that of a pure methanol solution by adding a little amount of camphor (1%) to the solution. The current density rose and reached a maximum value when the camphor concentration

(5%) increased. The current density of camphor in methanol solution is decreasing and possibly becoming lower than that of simply methanol, indicating that camphor in methanol solution is over saturated.

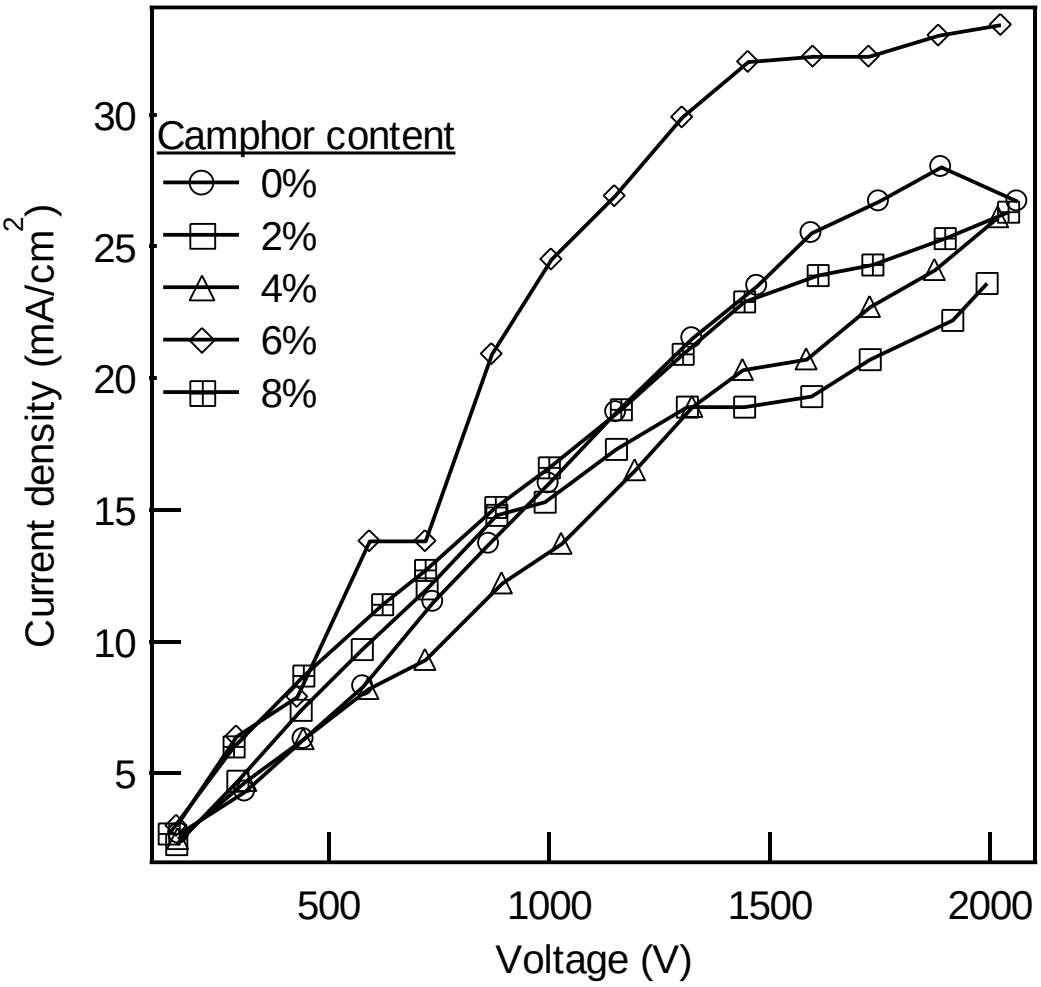

Fig. 4.4 Current density of the Si substrate as a function of applied voltage in response to methanol with different camphor concentrations (0%, 2%, 4%, 6% and 8%) [30]

For the Si substrate, the current density as a function of applied voltage is measured once again. The Si substrate's fluctuation in current density with applied voltage differs slightly from the Al and Cu substrates. **Fig. 4.4** depicts it. Camphor (2%) reduces current density at first, then continues to decline for another 4%. The current density increases with the addition of more camphor (6%) and reaches a maximum value, but it then falls with the addition of more camphor (8% and above).

4.3.1 Findings from current density using camphor in methanol

- By using camphor initially current density decreases from that of only methanol solution, then it increases and reaches to a maximum value, then again current density decreases by increasing camphor from the optimum percentage.
- Maximum current density was found:

- Al substrate containing 2% camphor in methanol solution.
- Cu substrate with 2% camphor in a methanol solution.
- For the Zn substrate, 5% camphor in methanol solution was used.
- For the Si substrate, 6% camphor in methanol solution was used.

4.4 Measurement of current density using CNT in methanol on Si substrate

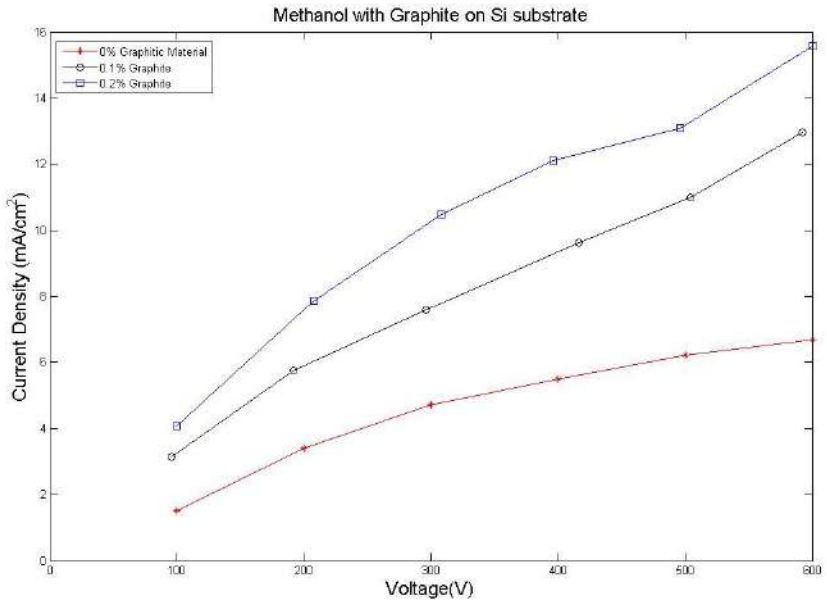

Fig. 4.5 Methanol with Graphite material on Si substrate [33]

Here in case of Graphite in Methanol solution we can notice a moderate current density before adding any Graphite material but after adding Graphite material the current density increases and it is higher in case of 0.2% graphite.

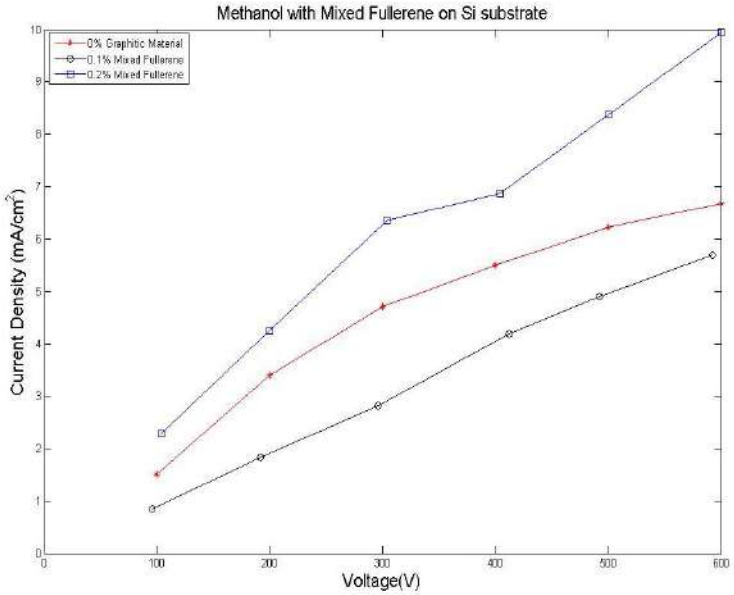

Fig. 4.6 Methanol with Mixed Fullerene on Si Substrate [33]

In case of Fullerene in Methanol solution we can notice a moderate current density before adding any Fullerene material but after adding Fullerene material the current density increases for 0.2% Fullerene and it decreases in case of 0.1% Fullerene.

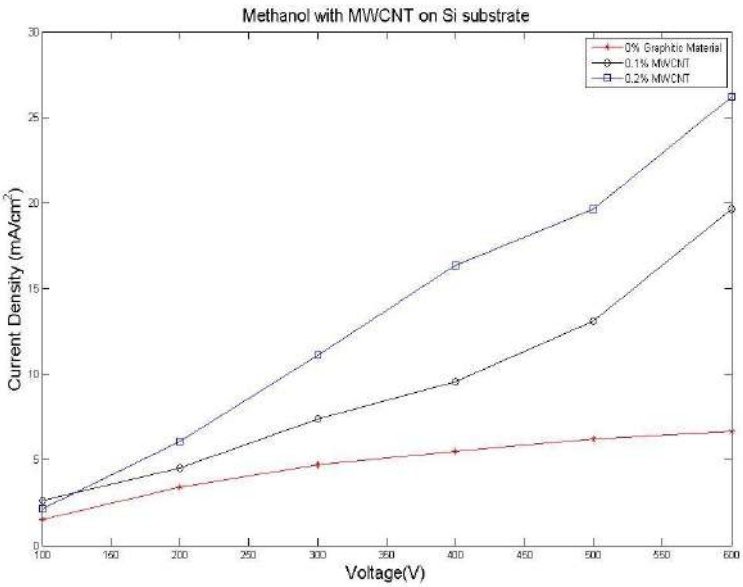

Fig. 4.7 Methanol with MWCNT on Si substrate [33]

In case of MWCNT in Methanol solution we can notice a moderate current density before adding any MWCNT material but after adding MWCNT material the current density increases and it is higher for 0.2% MWCNT.

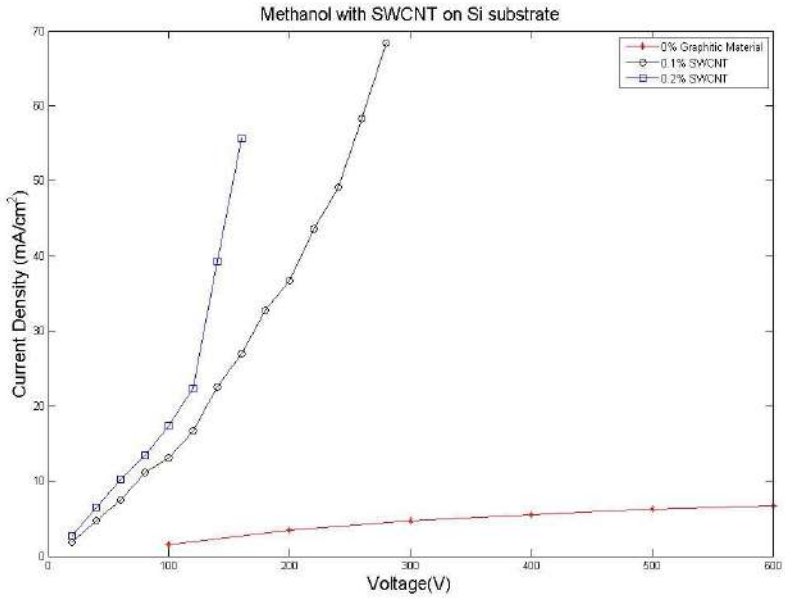

Fig. 4.8 Methanol with SWCNT on Si substrate [33]

For SWCNT in Methanol solution we can notice a moderate current density before adding any SWCNT material but after adding SWCNT material the current density increases and it is higher for 0.1% SWCNT.

4.4.1 Findings from current density using CNT in methanol on Si substrate

We detected a moderate current density in the liquid phase during electrodeposition from the graphs of current density employing CNT in methanol. However, as individual CNT components are incorporated into methanol, the current density rises. By increasing the amount of CNT materials in methanol, the current density also rises. Lowest current density was observed for Fullerene and maximum current density was observed for SWCNT.

4.5 Findings from current density using Camphor & CNT in methanol on Al, Cu, Zn & Si substrate

- For deposition by camphor higher current density was observed on Zn substrate.
- Current densities by deposition of CNT on Si substrate were higher than that of camphor.
- As substrate Si shows higher affinity to carbonic electrodeposition.

4.6 Characterization of deposited films by SEM analysis using camphor in methanol

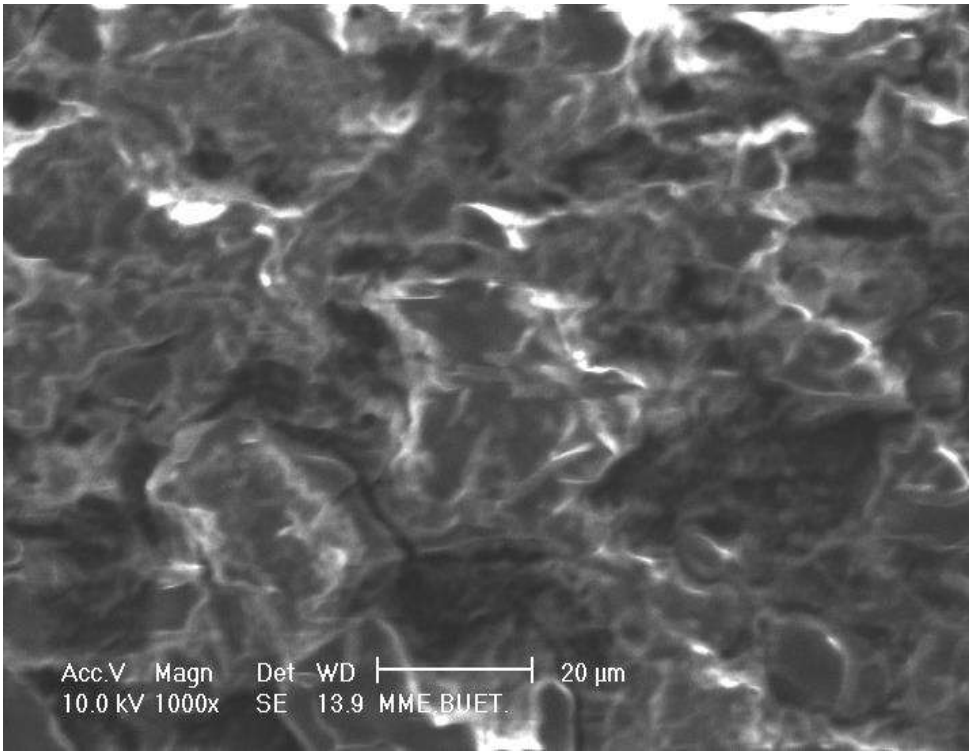

Fig. 4.9 SEM micrograph of the film deposited in 2% camphor in methanol solution on Al substrate [30]

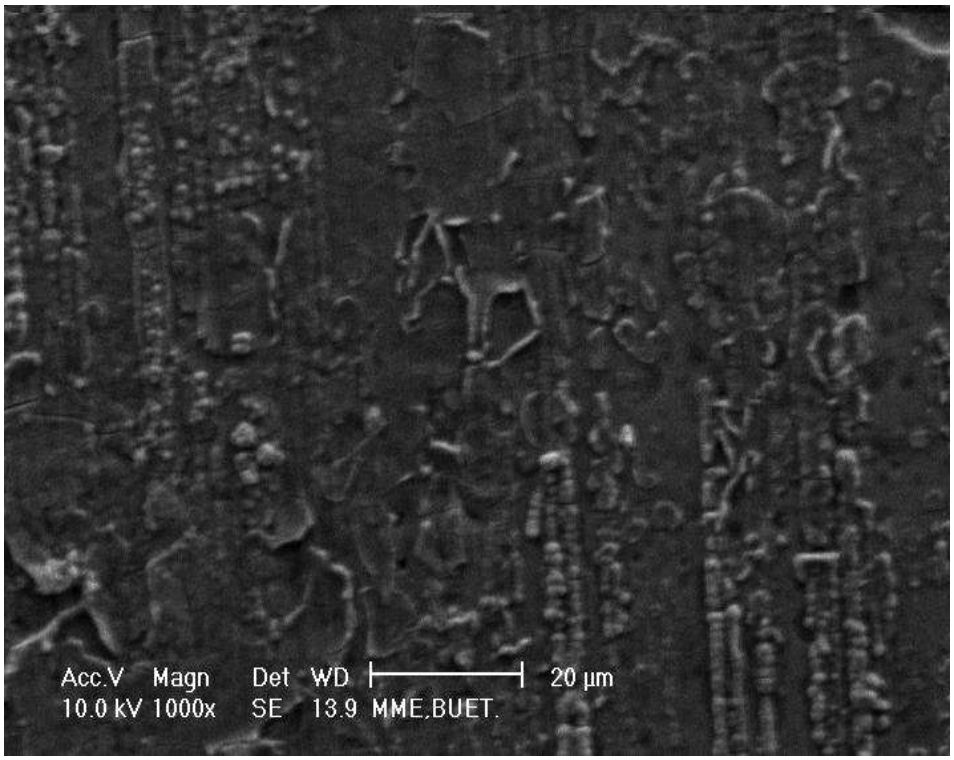

Fig. 4.10 SEM image of a film deposited on a Cu substrate in a 2 % camphor in methanol solution [30]

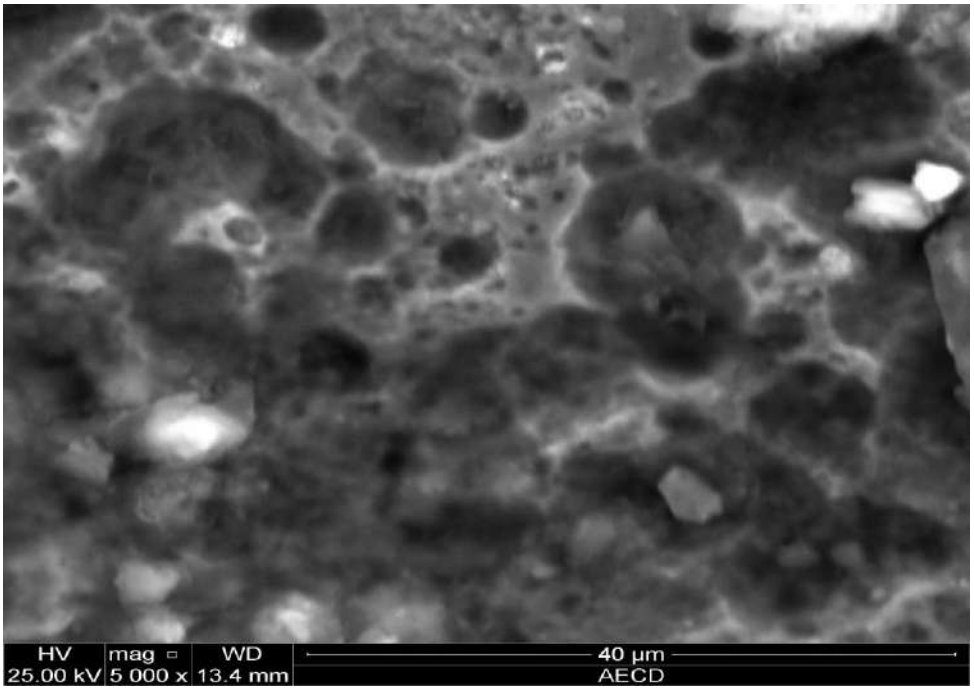

Fig. 4.11 SEM image of a coating deposited on a Zn substrate in a 2% camphor in methanol solution [34].

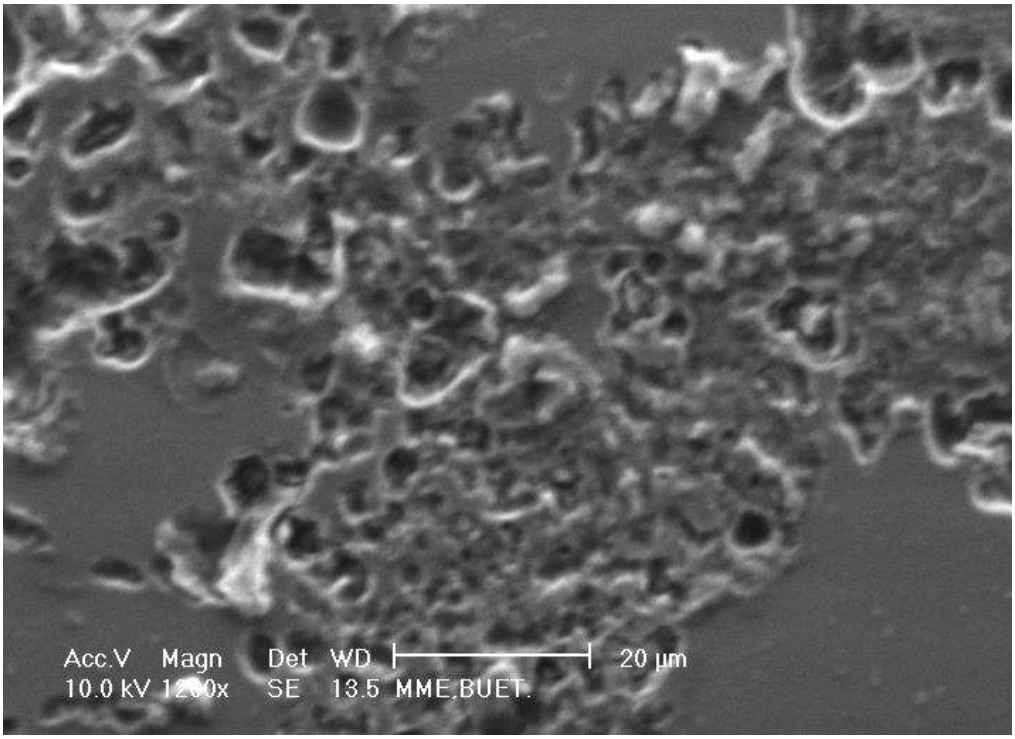

Fig. 4.12 SEM micrograph of the film deposited in 2% camphor in methanol solution on Si substrate [30]

We can see that there are differences in the micrographs of the electrodeposited films on different substrates, as detected by SEM micrographs, in these photographs of SEM

analysis found in prior research using camphor in methanol solution. For various percentages of camphor, micrographs of the same electrodeposited substrates reveal differences. As a result, the substrate type and camphor % have an impact on the creation of carbon thin films.

4.7 Characterization of deposited films by EDS analysis using camphor in methanol

Table 4.4: Data for Composition of Carbonic Films on Different Substrates (Al, Cu, Zn and Si) [30], [34].

Summary of EDS for Al, Cu, Zn & Si							
Substrates Deposited	Percentage of Camphor Used		Weight (%) of Chemicals Observed				
		Al	Cu	Zn	Si	C	O
Al	2%	87.79	0.00	0.00	0.00	12.21	0.00
Cu	2%	0.00	86.76	0.00	0.00	13.24	0.00
Zn	5%	0.00	0.00	88.64	0.00	9.21	2.15
Si	6%	0.00	0.00	0.00	78.85	21.15	0.00

Based on the aforementioned chemical study, there are evidence that some carbon films are present. The results in **Table 4.4** also shows that the proportion of carbon on the electrodeposited substrate is highest for Si substrate.

4.8 Characterization of deposited films by SEM analysis using CNT in methanol on Si substrate

From the previous works of carbon thin film deposition using CNT in methanol we can see that for the SEM analysis both electrodeposition and spin coating methods are conducted here. Now we will compare those results here.

4.8.1 Characterization of deposited films by SEM analysis using CNT in methanol on Si substrate by electrodeposition

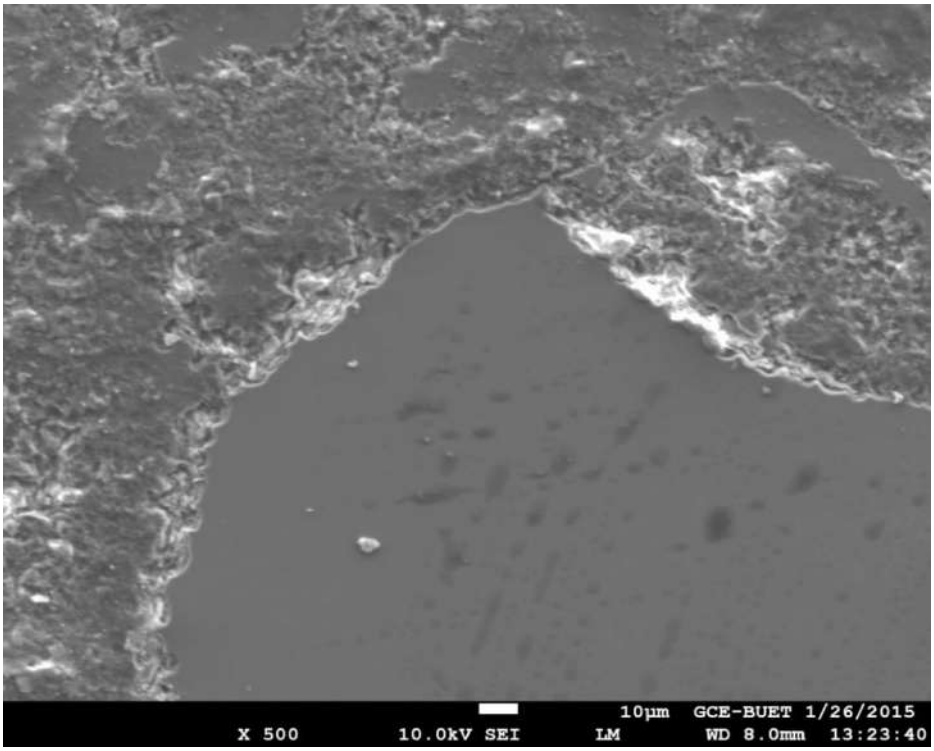

Fig. 4.13 SEM image of nanotube films deposited on Si with ED 0.2 % Fullerene [33]

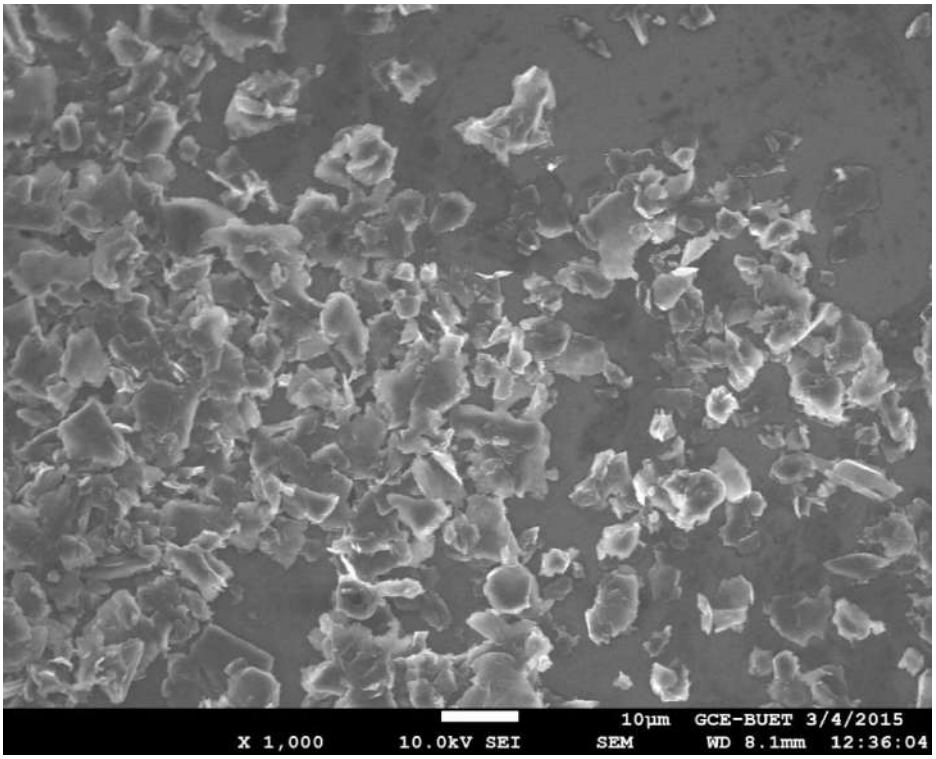

Fig. 4.14 SEM image of nanotube films deposited on Si with ED 0.2 % Graphite [33]

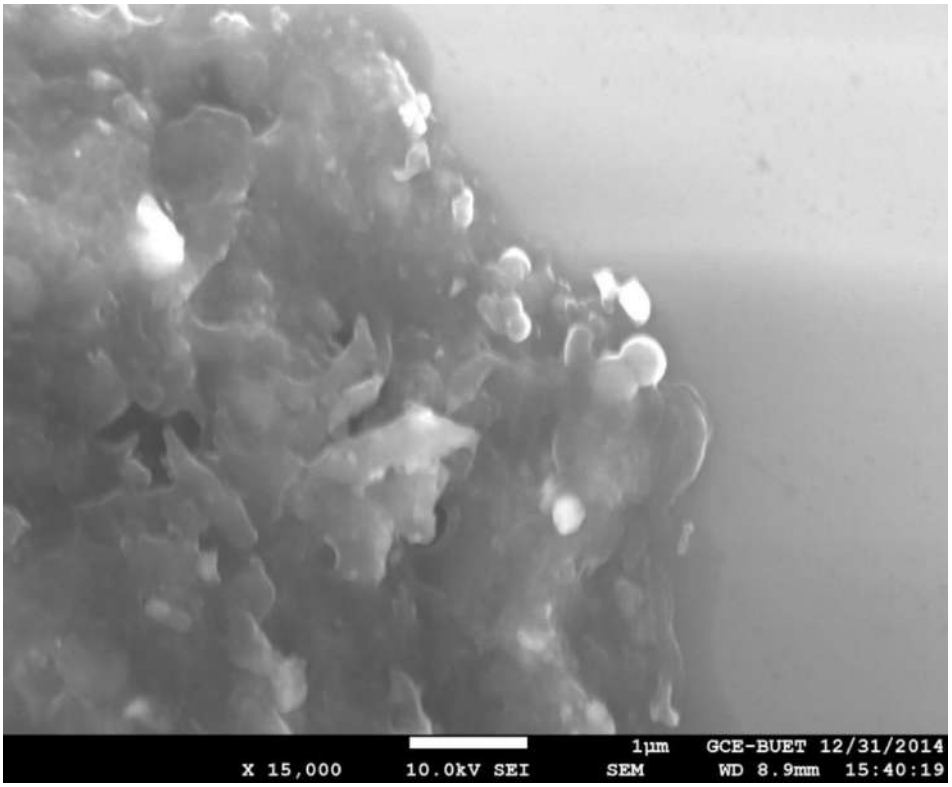

Fig. 4.15 SEM image of nanotube films deposited on Si with ED 0.2 % MWCNT [33]

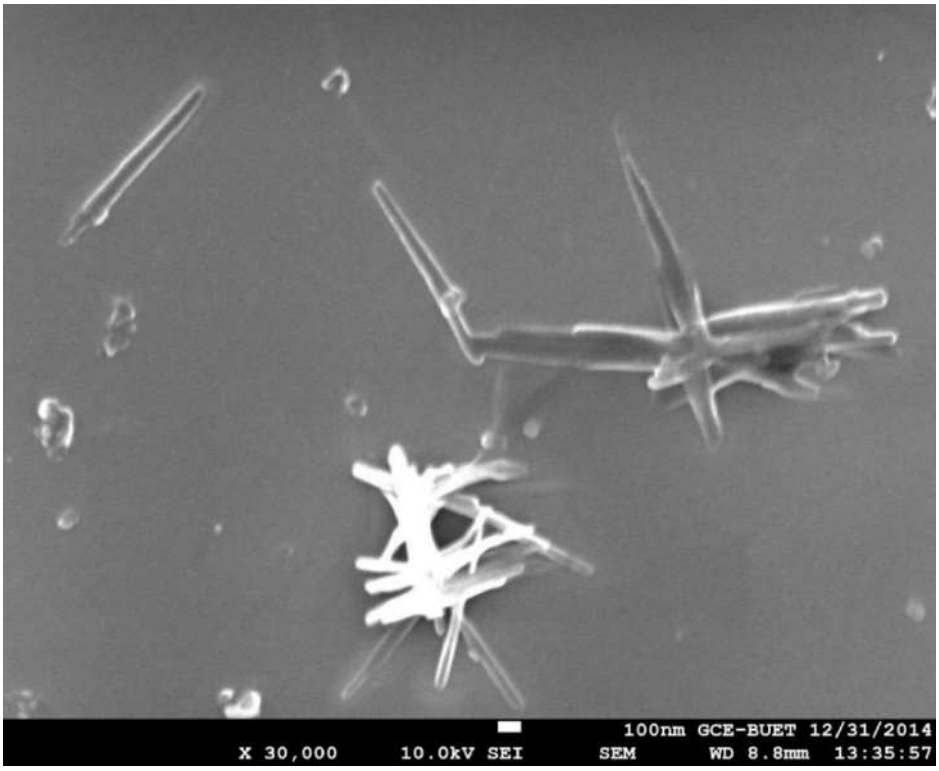

Fig. 4.16 SEM image of nanotube films deposited on Si with ED 0.2 % SWCNT [33]

4.8.2 Characterization of deposited films by SEM analysis using CNT in methanol on Si substrate by spin coating

Fig. 4.17 SEM image of nanotube films deposited on Si with SP 0.2 % Fullerene [33]

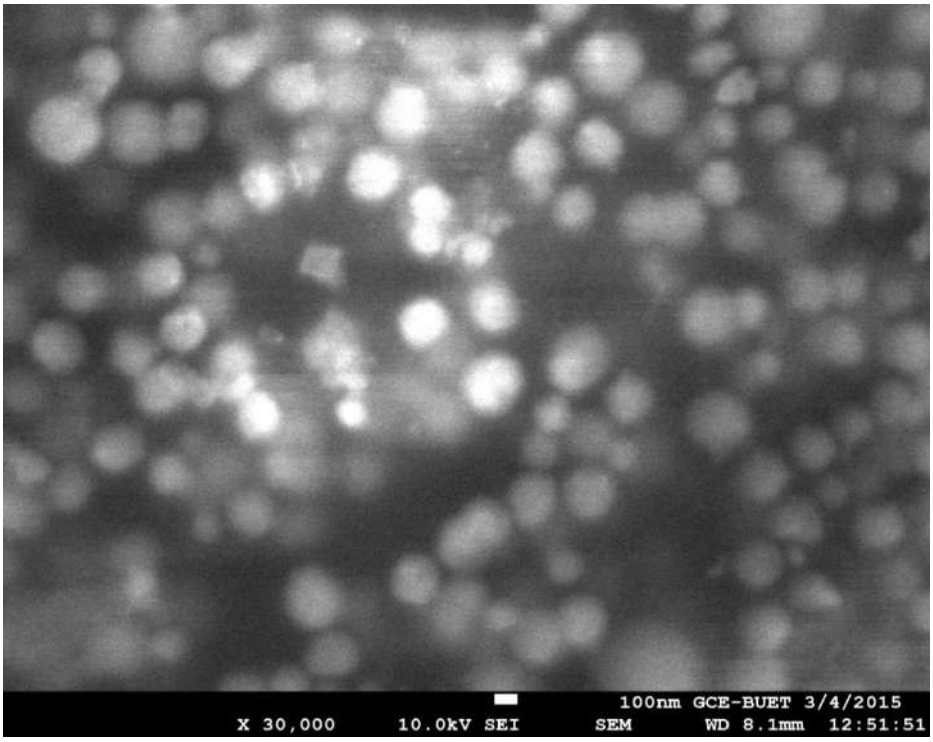

Fig. 4.18 SEM image of nanotube films deposited on Si with SP 0.2 % Graphite [33]

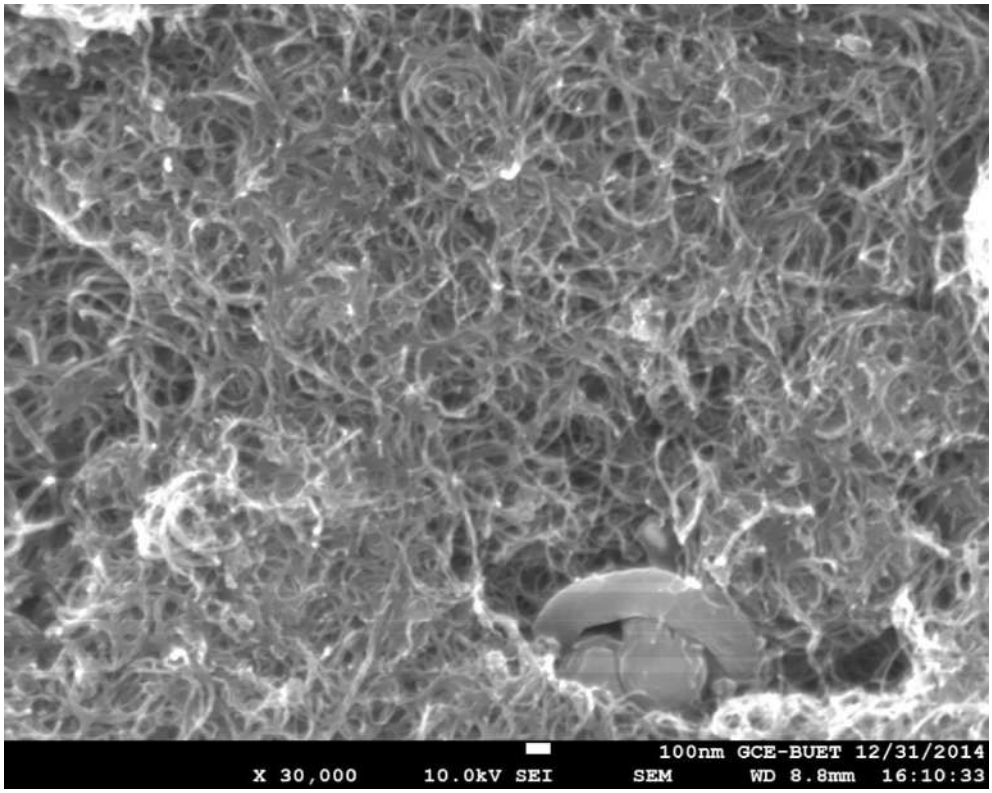

Fig. 4.19 SEM image of nanotube films deposited on Si with SP 0.2 % MWCNT [33]

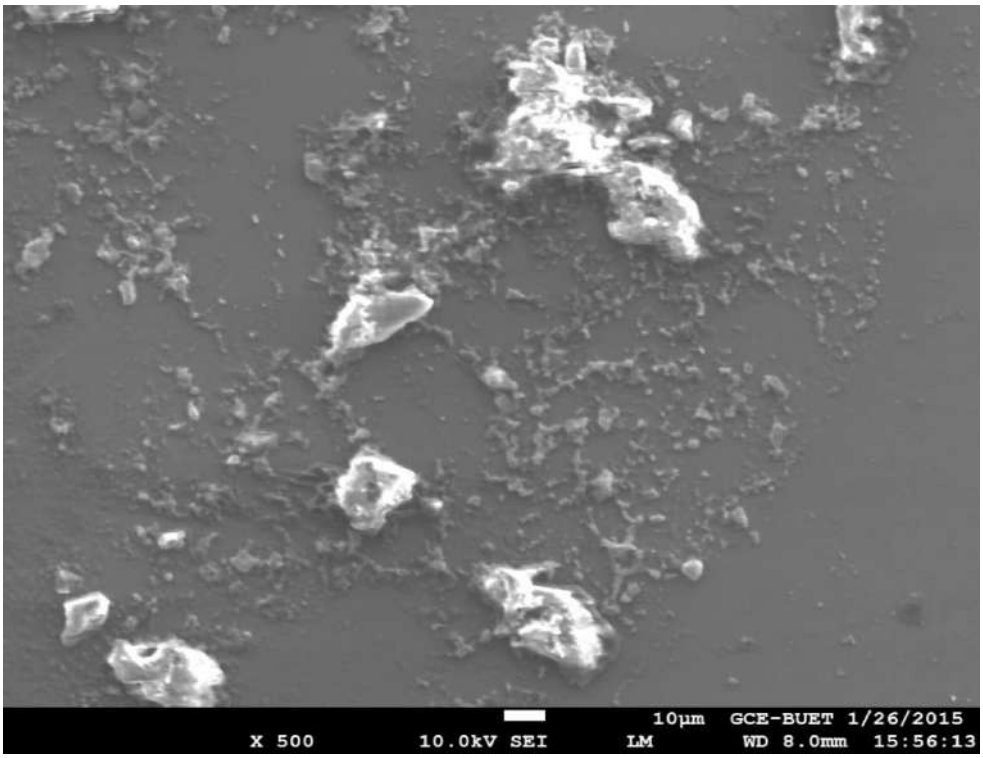

Fig. 4.20 SEM image of nanotube films deposited on Si with SP 0.2 % SWCNT [33]

When comparing the micrographs of electrodeposited and spin coated films on Si substrates to pure Si substrates and films deposited in just methanol solution, we noticed that there are differences. Micrographs of the identical electrodeposited and spin coated substrates show changes for varying percentages of CNT. The production of carbon thin films is influenced by CNT variation. In both cases electrodeposition and spin coating MWCNT shows some nanowires as the mentioned dimension is 1 μm and the size of the wire will be definitely within 100 nm.

4.8.3 Findings from SEM analysis

- In SEM, the effect of Methanol and other carbonic materials may be seen.
- Nanowires and nanoparticles are observed in CNT film on Si.
- Spin coating shows better nano properties compared to Electrodeposition.

4.9 Characterization of deposited films by EDS analysis using CNT in methanol on Si substrate

From the previous works of carbon thin film deposition using CNT in methanol we can see that for the EDS analysis both electrodeposition and spin coating methods are conducted here. We will compare the results using the same pictures found in SEM analysis.

4.9.1 Characterization of deposited films by EDS analysis using CNT in methanol on Si substrate by electrodeposition

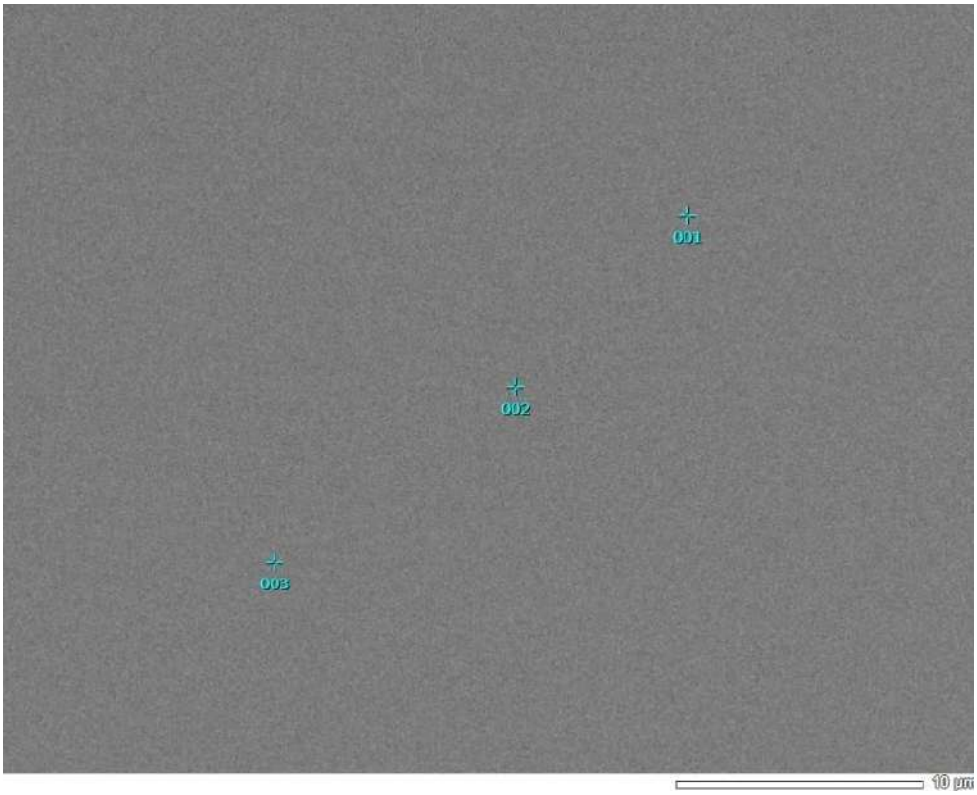

Fig. 4.21 Pure Silicon substrate observed in EDS [33]

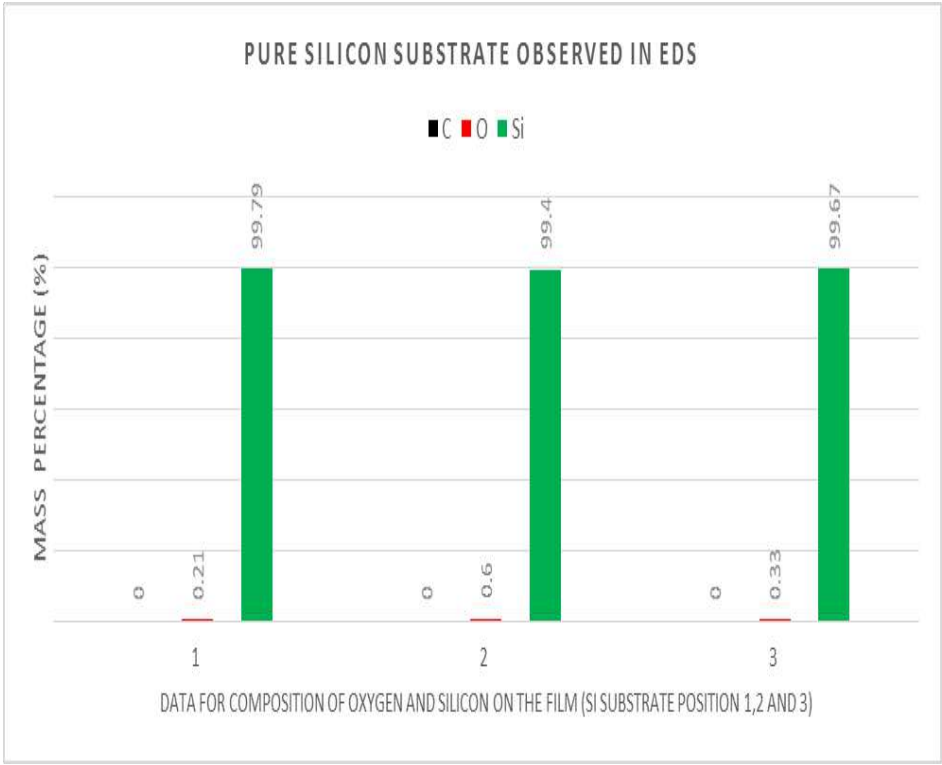

Fig. 4.21.1 Bar chart of mass (%) of Carbon, Oxygen and Silicon of the film on Si substrate [33]

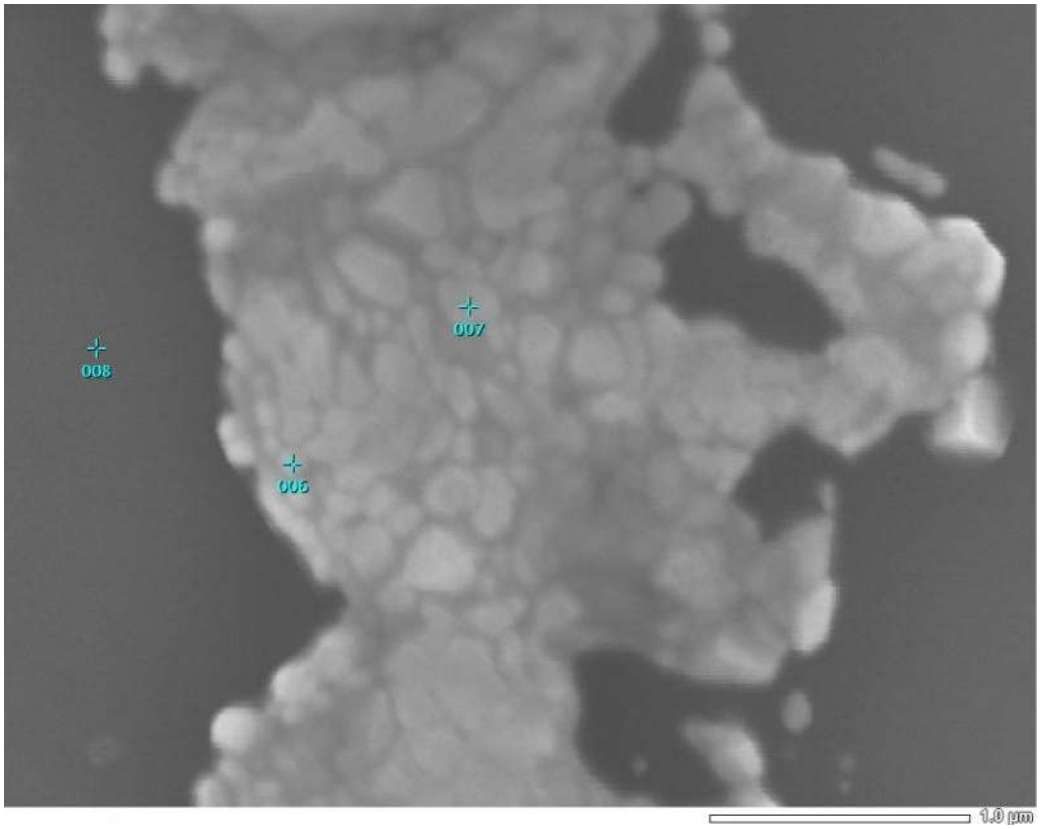

Fig. 4.22 Film using Only Methanol on Si substrate observed in EDS [33]

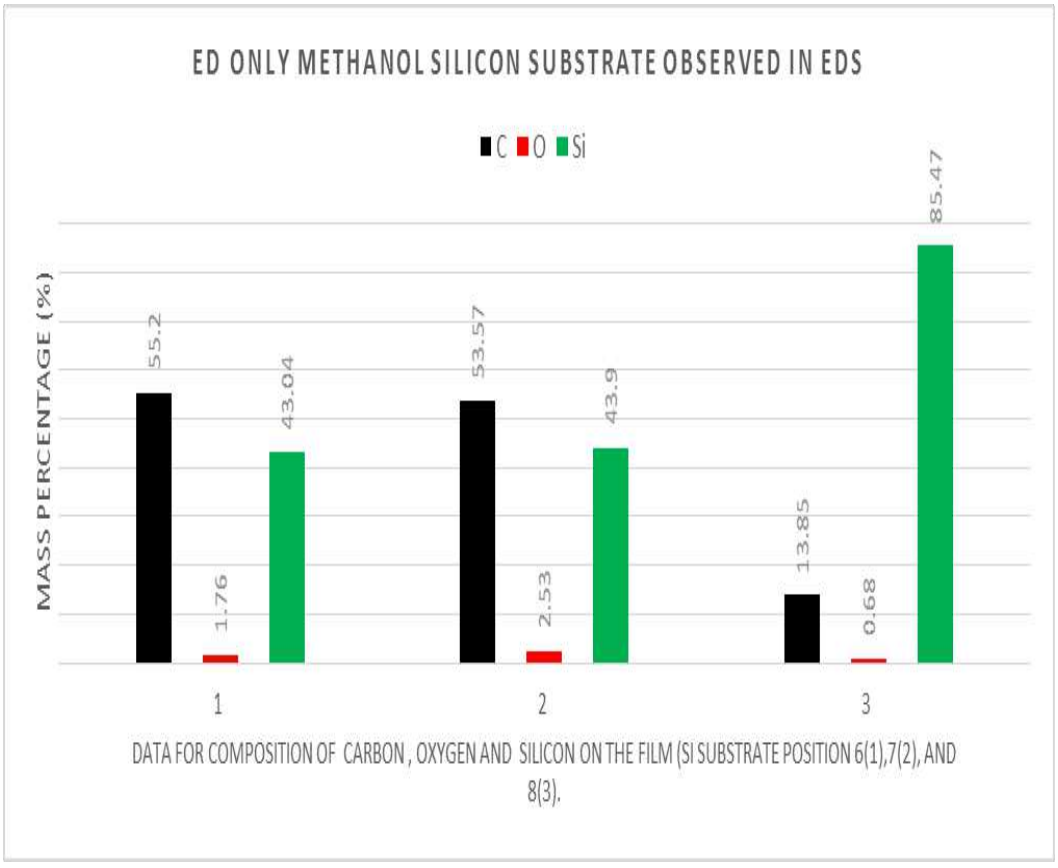

Fig. 4.22.1 Bar chart of mass (%) of Carbon, Oxygen and Silicon of the film on Si substrate [33]

Fig. 4.23 EDS observations of nanotube films formed on Si with ED 0.2 % Fullerene [33]

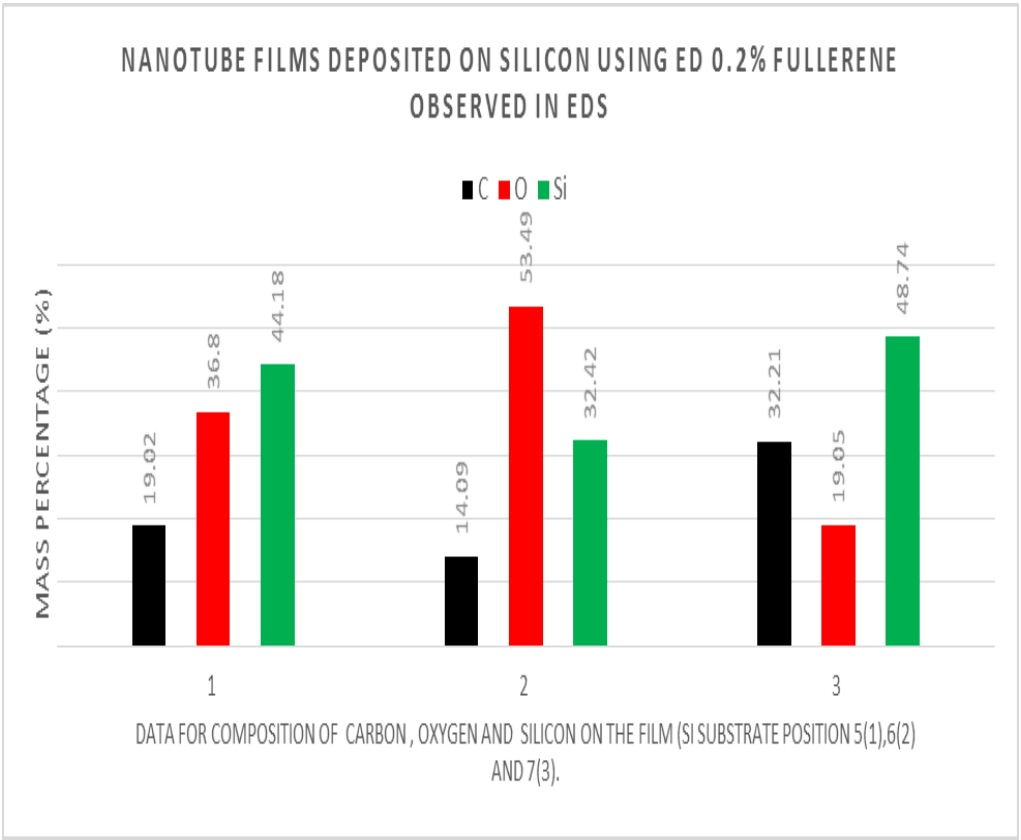

Fig. 4.23.1 Bar chart of mass (%) of Carbon, Oxygen and Silicon of the film on Si substrate [33]

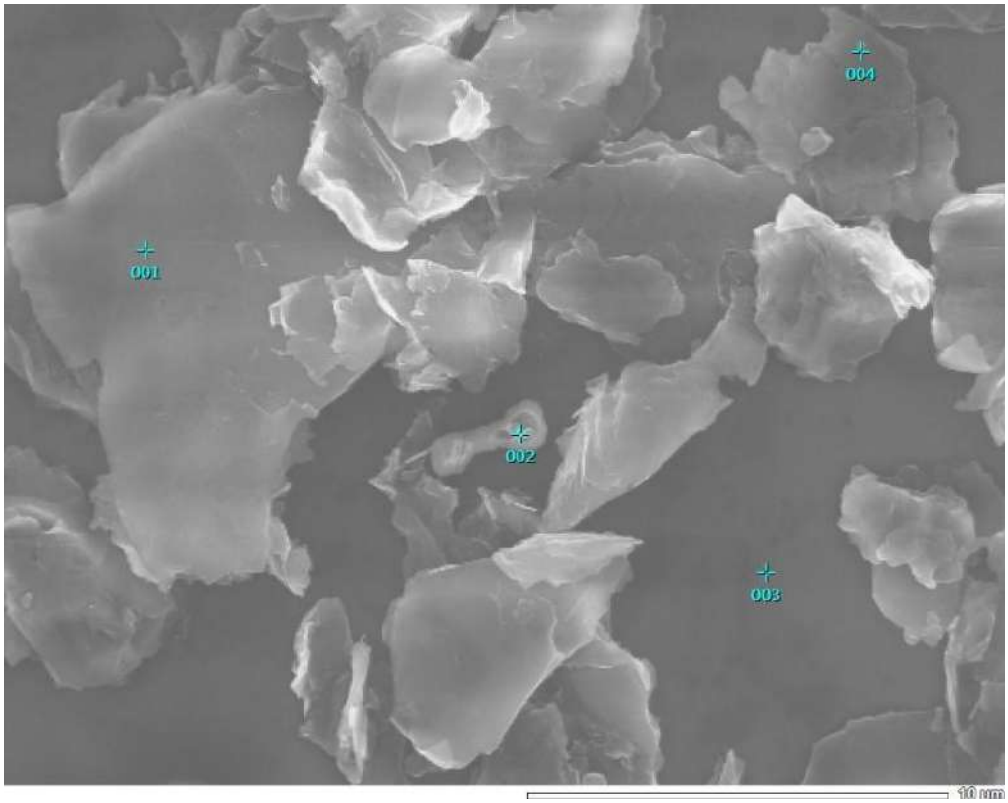

Fig. 4.24 EDS observations of nanotube films formed on Si with ED 0.2 % Graphite [33]

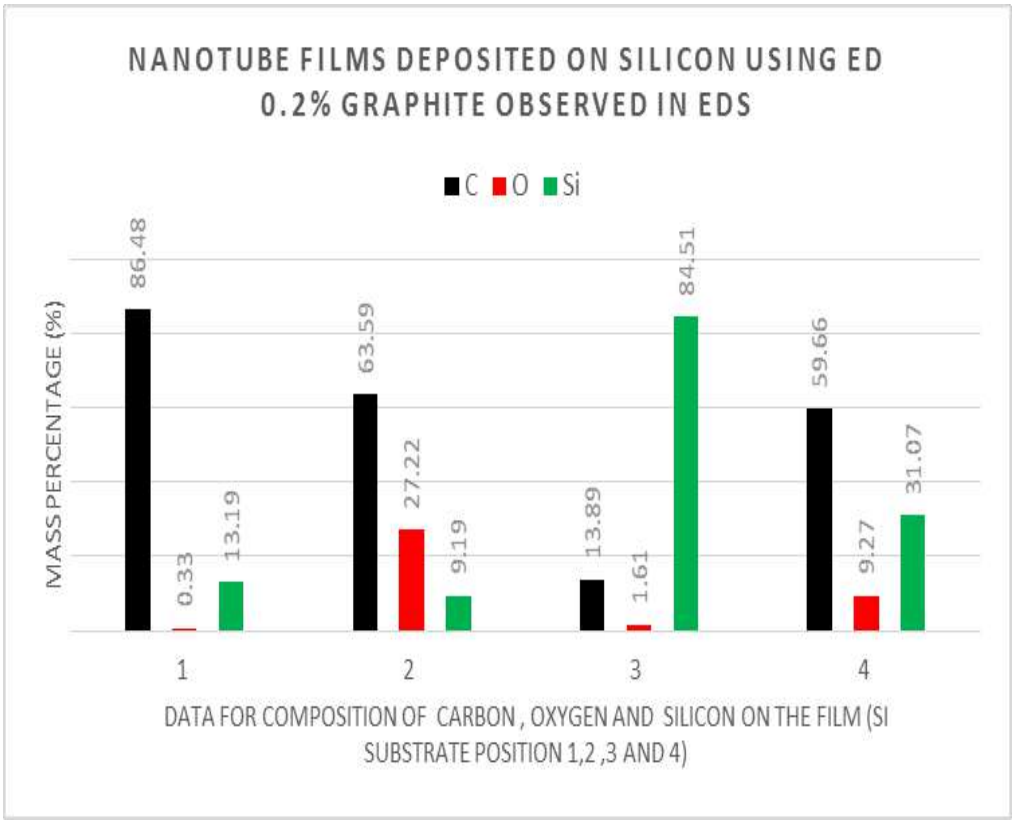

Fig. 4.24.1 Bar chart of mass (%) of Carbon, Oxygen and Silicon of the film on Si substrate [33]

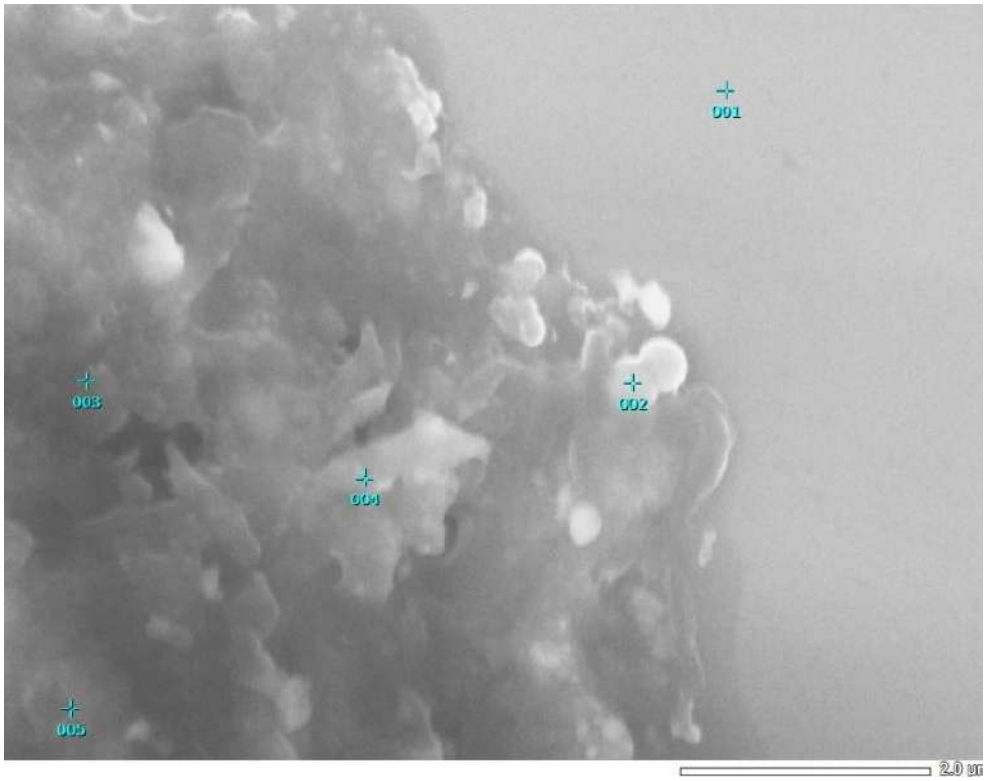

Fig. 4.25 EDS observations of nanotube films formed on Si with ED 0.2 % MWCNT [33]

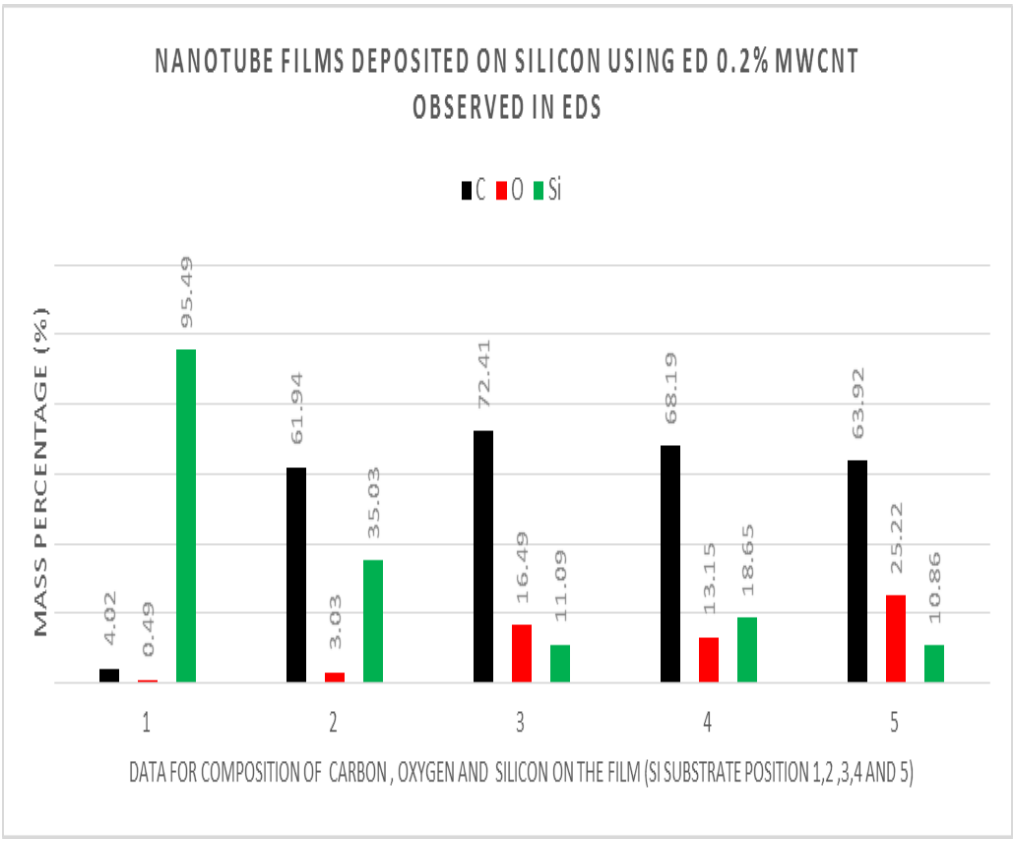

Fig. 4.25.1 Bar chart of mass (%) of Carbon, Oxygen and Silicon of the film on Si substrate [33]

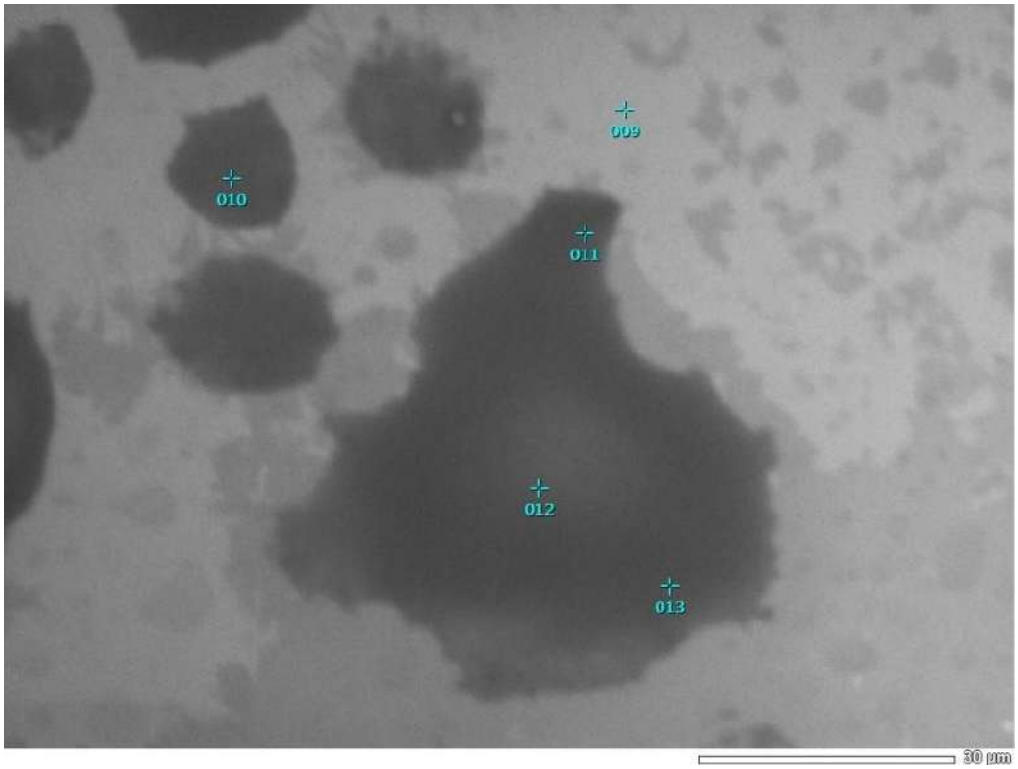

Fig. 4.26 EDS observations of nanotube films formed on Si with ED 0.2 % SWCNT [33]

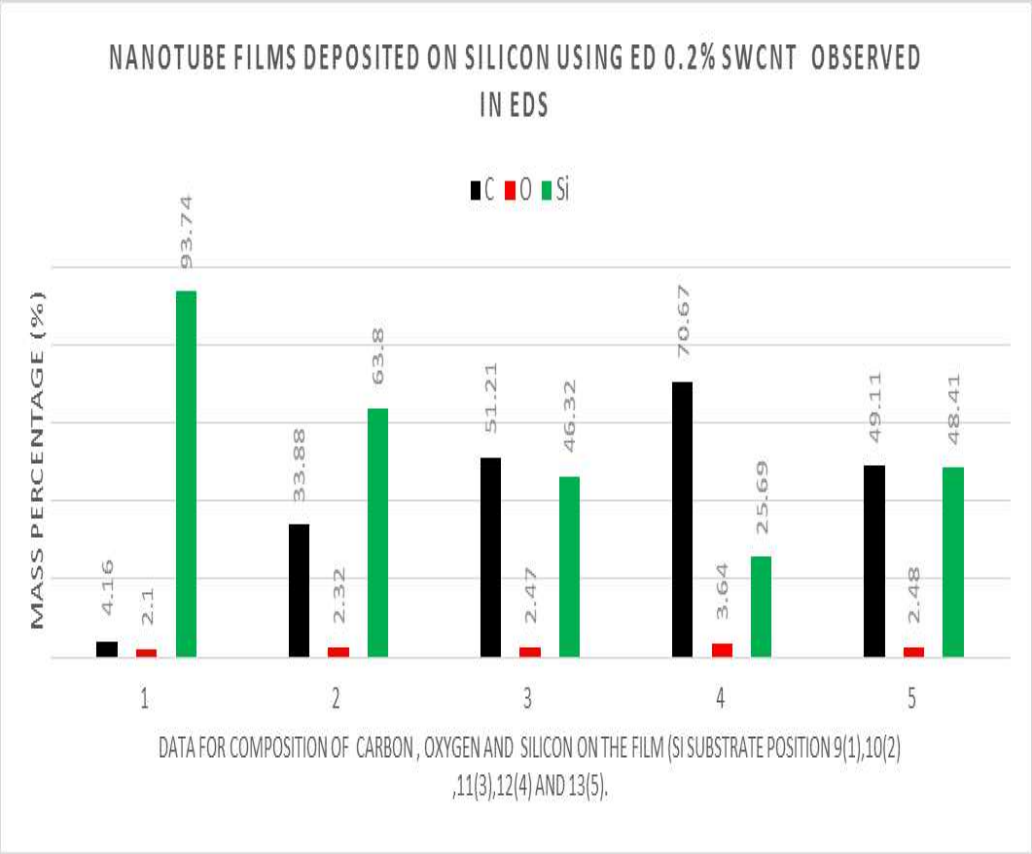

Fig. 4.26.1 Bar chart of mass (%) of Carbon, Oxygen and Silicon of the film on Si substrate [33]

4.9.2 Characterization of deposited films by EDS analysis using CNT in methanol on Si substrate by spin coating

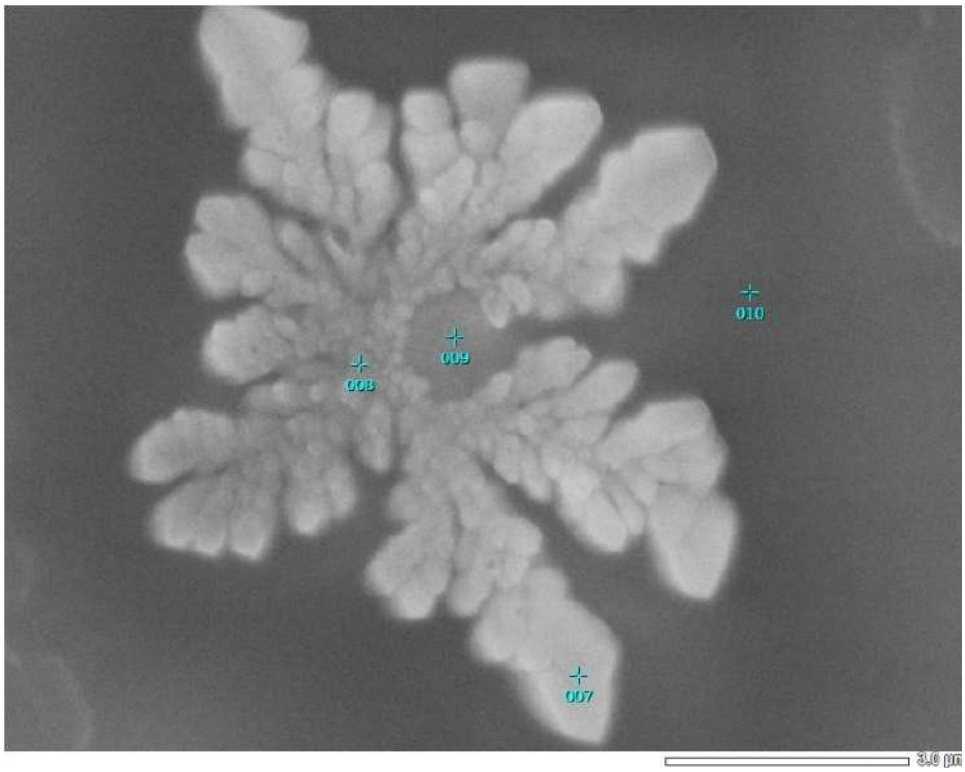

Fig. 4.27 Film using Only Methanol on Si substrate observed in EDS [33]

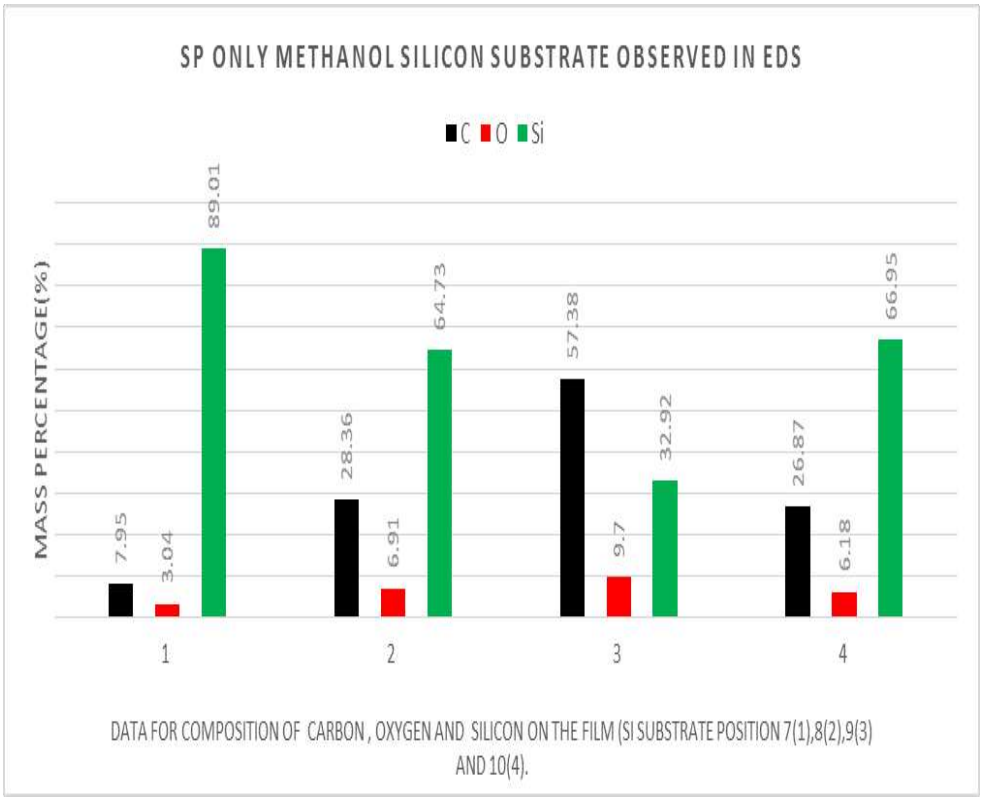

Fig. 4.27.1 Bar chart of mass (%) of Carbon, Oxygen and Silicon of the film on Si substrate [33]

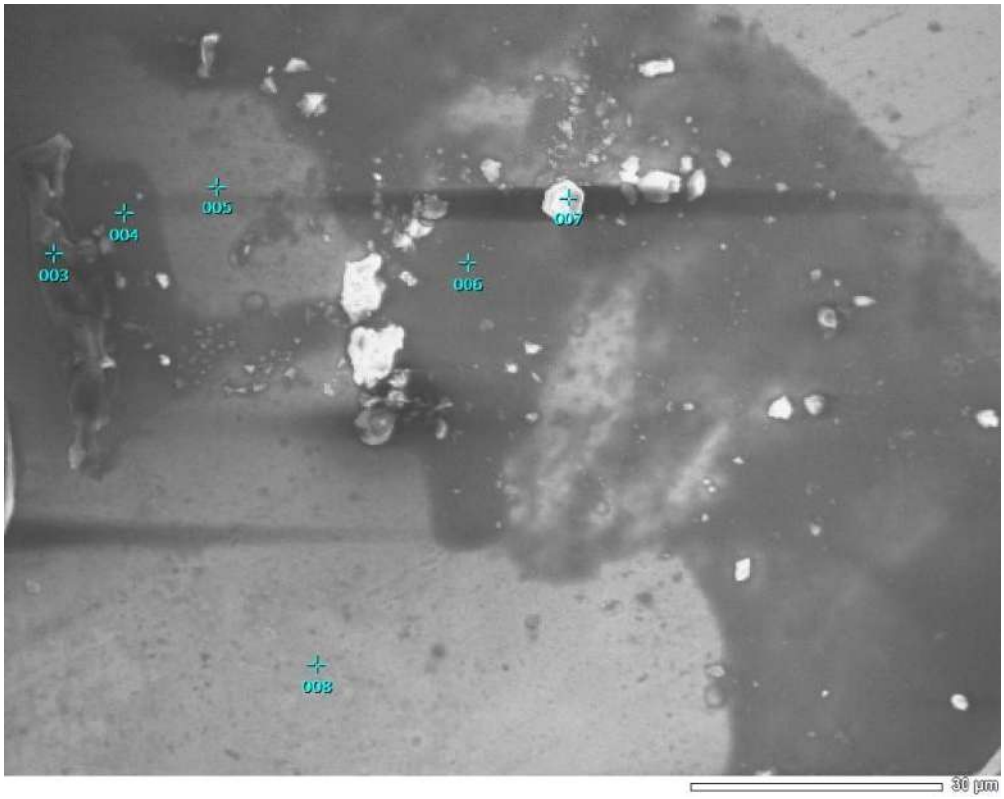

Fig. 4.28 EDS observations of nanotube films formed on Si with SP 0.2 % Fullerene [33]

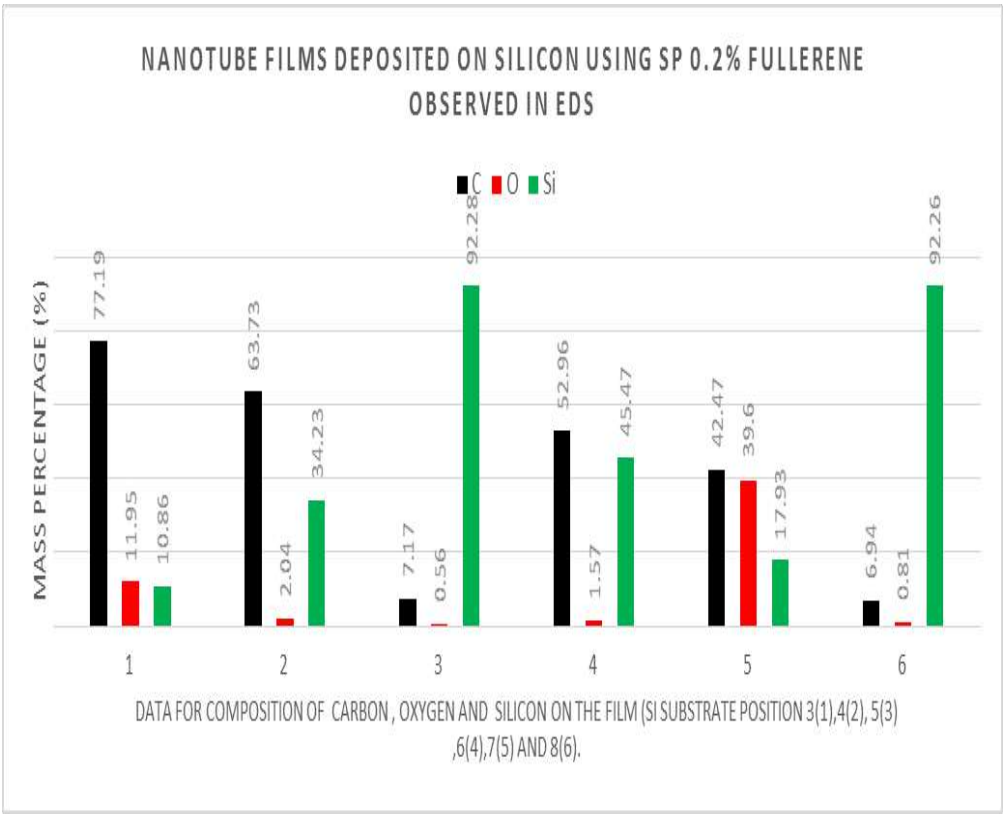

Fig. 4.28.1 Bar chart of mass (%) of Carbon, Oxygen and Silicon of the film on Si substrate [33]

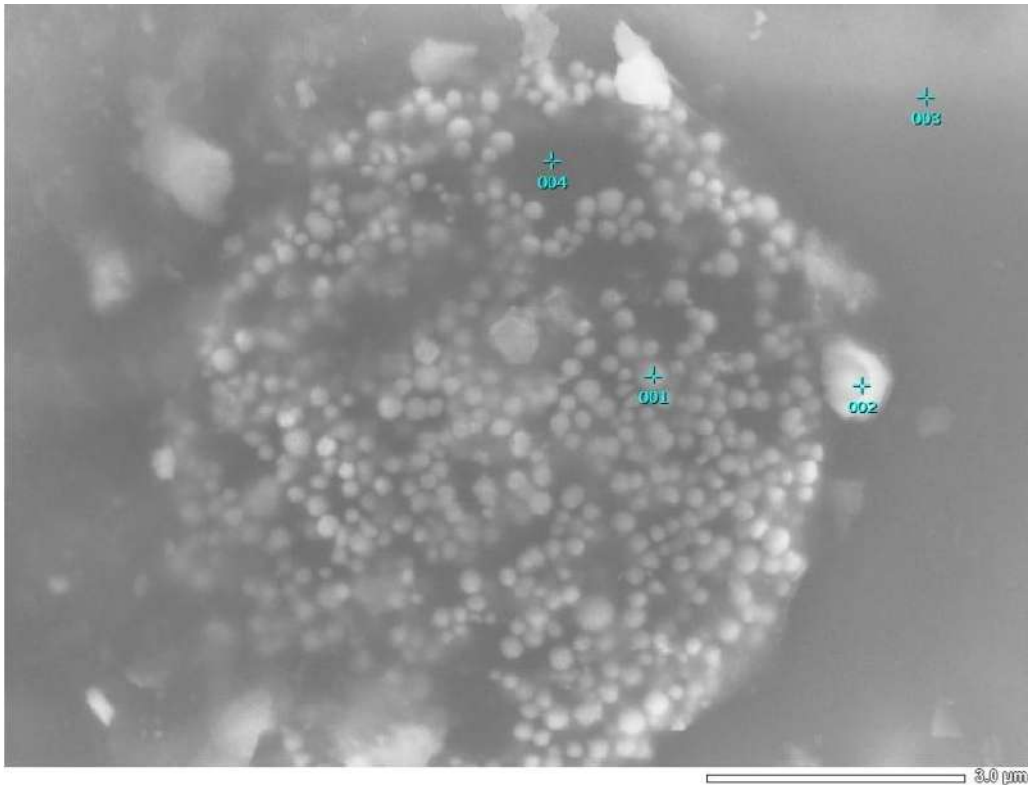

Fig. 4.29 EDS observations of nanotube films formed on Si with SP 0.2 % Graphite [33]

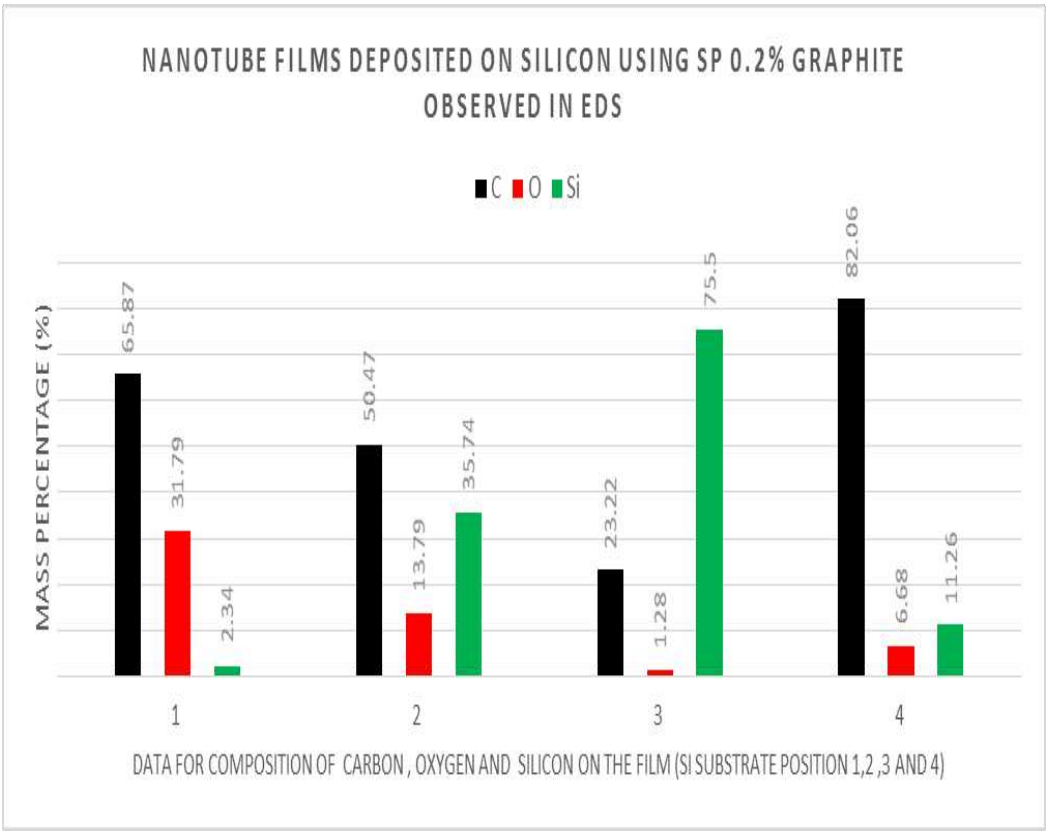

Fig. 4.29.1 Bar chart of mass (%) of Carbon, Oxygen and Silicon of the film on Si substrate [33]

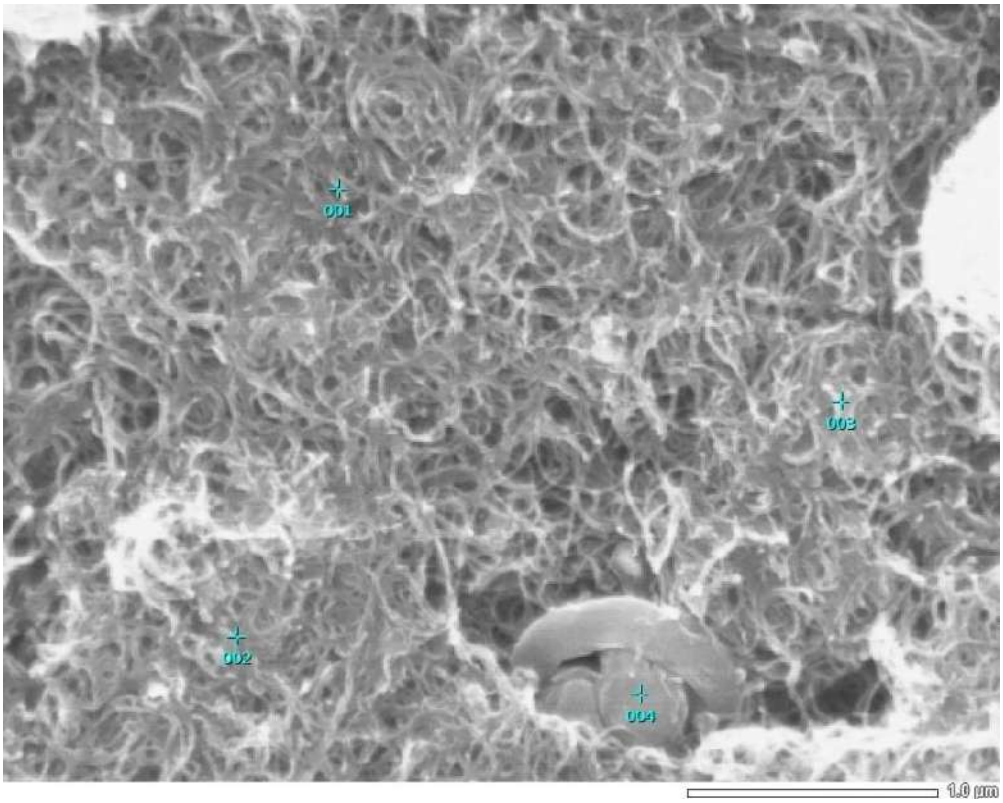

Fig. 4.30 EDS observations of nanotube films formed on Si with SP 0.2 % MWCNT [33]

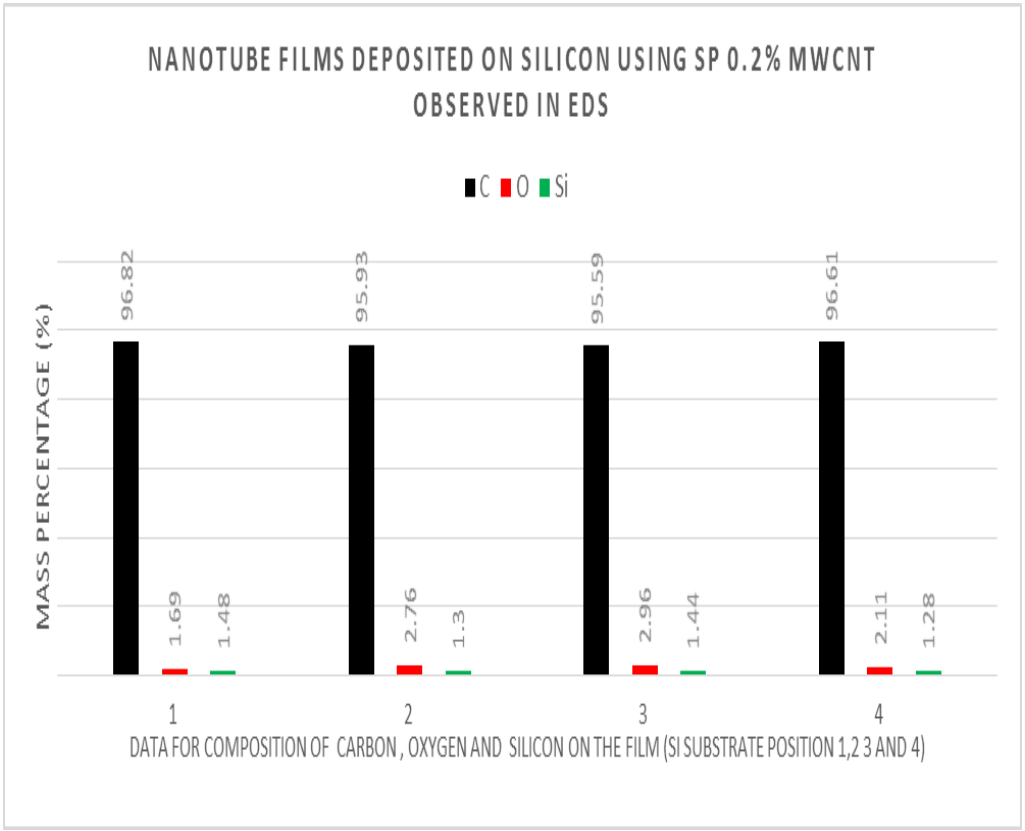

Fig. 4.30.1 Bar chart of mass (%) of Carbon, Oxygen and Silicon of the film on Si substrate [33]

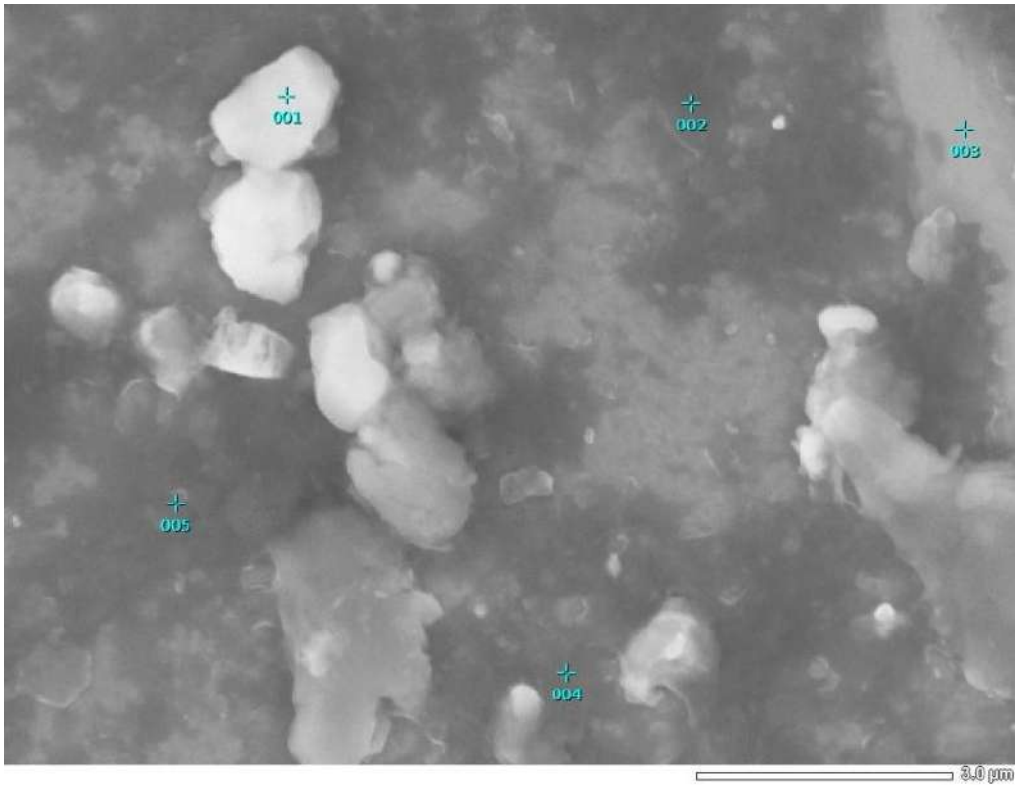

Fig. 4.31 EDS observations of nanotube films formed on Si with SP 0.2 % SWCNT [33]

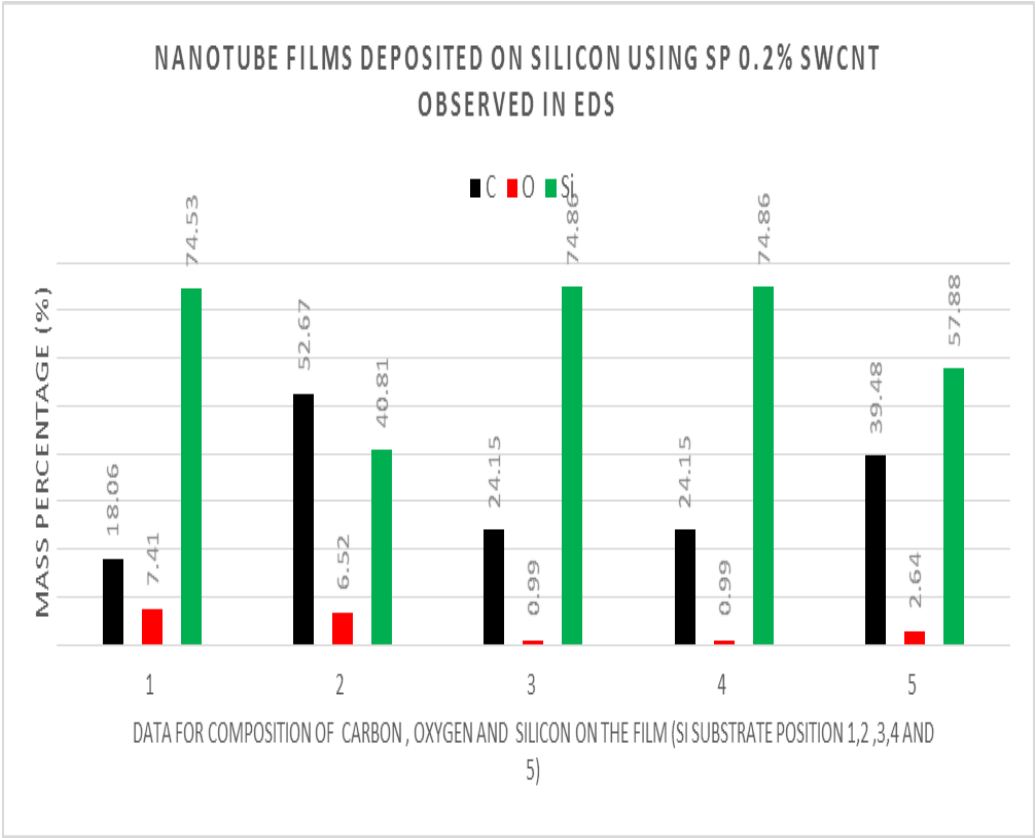

Fig. 4.31.1 Bar chart of mass (%) of Carbon, Oxygen and Silicon of the film on Si substrate [33]

There are some signs that carbonic films are generated based on the above bar charts. The bar chart also shows varying amounts of carbon, oxygen, and silicon at various material positions. The percentage of carbon varies at many positions of the films, which is extremely evident to us. It might be totally carbonic film, or it can be composed of carbon, silicon, and oxygen. In case of pure Si there are no signs of carbon. In case of MWCNT both in electrodeposition and spin coating where there are nanowires are showing in the SEM pictures we can see in EDS analysis that in several positions the carbon contents are higher and in spin coating almost the entire percentage is carbon.

4.9.3 Findings from EDS analysis

- Carbonic films are observed in different substrates.
- Silicon shows higher affinity to carbon than Al, Cu and Zn.
- Carbon percentage of the electrodeposited films were higher for the nano carbonic materials compared to camphor.
- In case of films using MWCNT on Si substrate (both Electrodeposition and Spin Coating) highest percentage of carbon were observed.

Chapter 5

CONCLUSION

5.1 Conclusion

Optoelectronic properties can be tuned using carbonic materials with methanol solution. Changes of P^H of electrolytes before and after deposition indicates any chemical changes on the substrates. Current density during liquid phase electrodeposition can be controlled by variation of carbonic materials. For camphoric methanol solution an optimum percentage of camphor gives maximum current density on several substrates (Al, Cu, Zn & Si). Current density by CNT material on Si substrate is higher than that of Camphor. Carbon percentage of electrodeposited films are higher by CNT compared to Camphor. In case of films using MWCNT on Si substrate (both Electrodeposition and Spin Coating) highest percentage of carbon were observed. Nanowires and Nanoparticles are observed in CNT film on Si substrate. Spin Coating shows better nano properties compared to Electrodeposition. Percentage of carbon of the deposited films is higher on Si (both for Camphor and other CNT materials) compared to other substrates (Al Cu, Zn) therefore Si is showing higher affinity to Carbon.

5.2 Future Development

- FTIR spectroscopy can be used to analyze the bonding types of thin films.
- For a better understanding of nanomaterials in thin films, transmittance/reflectance can be measured using UV-VIS-NIR spectroscopy.

REFERENCES

[1] M. S. Dresselhaus, G. Dresselhaus and P. C. Eklund, "Science of fullerenes and carbons," *Academic Press. Inc.*, 1996

[2] S. M. Mominuzzaman, T. Soga, T. Jimbo, and M. Umeno, "Camphoric carbon soot: a new target for deposition of diamond-like carbon films by pulsed laser ablation," *Thin Solid Films*, vol. 376, pp. 1-4, 2000.

[3] H.W. Kroto, J.R. Heath, S.C. O'Brien, R.F. Curl, R.E. Smalley, C60: buckminsterfullerene, Nature 318 (1985) 162.

[4] S.Iijima, Helical microtubules of graphitic carbon, Nature (London) 354 (1991) 56.

[5] S.Iijima, T. Ichihashi, Single-shell carbon nanotubes of 1-nm diameter, Nature (London) 363 (1993) 603.

[6] D.S. Bethune, C.H. Kiang, M.S. de Vries, G. Gorman, R. Savoy, J. Vazquez, R. Beyers, Cobalt-catalysed growth of carbon nanotubes with single-atomic-layer walls, Nature (London) 363 (1993) 605.

[7] G. Overney, W. Zhong, D. Toma´nek, Structural rigidity and low frequency vibrational modes of long carbon tubules, Z. Phys. D 27 (1993) 93–96.

[8] A.G. Rinzler, J.H. Hafner, P. Nikolaev, L. Lou, S.G. Kim, D. Tomanek, P. Nordlander, D.T. Colbert, R.E. Smalley,Unraveling nanotubes: field emission from an atomic wire, Science 269 (1995) 1550.

[9] S. M. Mominuzzaman, K. M. Krishna, T. Soga, T. Jimbo and M. Umeno, "Raman Spectra of Ion Beam Sputtered Amorphous Camphoric Carbon Thin Films", *Carbon*, vol. 38, 2000, pp. 127-131.

[10] S M Mominuzzaman, H Ebishu, T Soga, T Jimbo and M Umeno, "Phosphorus Doping and Defeat Studies of Diamond Like Carbon Films by Pulsed Laser Deposition Using Camphoric Carbon Target, *Diamond And Related Materials*, Vol. 10, pp 948-988, 2000.

[11] R. C. Haddon and S.-Y. Chow, Hybridization as a metric for the reaction coordinate of the chemical reaction: concert in chemical reactions, Pure Appl. Chem. 71, 289–294 (1999).

[12] P. Koidl, C. Wild, B. Dischler, J. Wagner, and M. Ramsteiner, "Preparation and mechanical properties of composite diamond-like carbon thin films", *Mater. Sci. Forum*, vol. 1, pp. 52-53, 1989.

[13] J C Angus, P Koidl and S Domiz in Plasma Deposited Thin Films, *Ed. J. Mort.* (Crc Ss, 1986)

[14] Y Catherine in Diamond and Diamond Like Carbon Filmed R E Clausinget Al (Plenum 1991) P 193

[15] Aisenberg and R. Chabot, "New radio frequency technique for deposition of hard carbon films", *J. Appl. Phys.* Vol. 42, pp. 2953, 1971.

[16] H Vora, T J Moravee, "Plasma deposition and etching of diamond-like carbon films", *J. App. Phys.* Vol. 52, pp. 6151, 1981.

[17] T. Motri and Y. Namba, “Surface Acoustic Wave Properties of Diamond-like Carbon Thin Films,” *J. Vac. Sci. Technol. A1,* vol. 23, pp. 5, 1983.

[18] HR Kaufman, “Technology of ion beam sources used in sputtering,” *J. Vac. Sci. Technol.,* vol. 15, pp. 272, 1978.

[19] C. B. Collins, F. Davanloo, F. R. Jandeer, T. J. Lee an C. B. Collins, *J. App. Phys.* 67 2081 (1990); *J. Matres* 5 298(1990).

[20] J Cuomo, J P Doyle, J Bruley, J C Liu, *App. Phys.* Lett. 58 466 (1991)

[21] T. Motri and Y. Namba, “Surface Acoustic Wave Properties of Diamond-like Carbon Thin Films,” *J. Vac. Sci. Technol. A1,* vol. 23, pp. 5, 1983.

[22] N Savvides, Jap. Ahys.55 4232 (1984).

[23] L Holland and S M Ojha, *Thin Solid Films* 58, 107(1979)

[24] P. Koidl, C. Wild, B. Dischler, J. Wagner, and M. Ramsteiner, “Preparation and mechanical properties of composite diamond-like carbon thin films”, *Mater. Sci. Forum,* vol. 1, pp. 52-53, 1989.

[25] C Weissmantel Etat, *Thin Solid Films* 63 315 (1979).

[26] A Wangendristel and Y Wang “An Introduction to Physics and Technology of Thin Films”, *World Scientific Publishing Co.* Singapore.

[27] Md. Shafiqul Islam, "Spectral Photo Response Characteristics of N Carbon / P Silicon Heterostructure," M. Sc. Thesis Department Of Electrical and Electronic Engineering, BUET, Dhaka, Bangladesh, 2002.

[28] Sunil Kumar, “Characteristics of bonding structures of diamond-like carbon films deposited by radio frequency,” Appl. Phys., vol. 58, pp. 1836-1838, 1991.

[29] spin-coating, Access date: 24 November, 2021, Retrieved from: https://www.ossila.com/pages/spin-coating

[30] Muhammad Athar Uddin, Md. Shamimul Haque Choudhury and Sharif M Mominuzzaman, "Characterization of Carbon Thin Films Electrodeposited on Aluminium, Copper and Silicon Substrates," 6th International Conference on Electrical and Computer Engineering ICECE 2010, pp. 206-209, 18-20 December 2010, Dhaka, Bangladesh.

[31] Muhammad Athar Uddin, T. Soga and Sharif M Mominuzzaman, “Characterization of Spincoated Multiwall Carbon Nanotube Films on Silicon Substrates” 9th International Conference on Electrical and Computer Engineering (ICECE), 2016, 20-22 December 2016, Dhaka, Bangladesh.

[32] Mohammad Wahidur Rahman, Muhammad Athar Uddin, Ahmedullah Aziz, Tanvir Mustofa, Zahid Hasan Mahmood, T. Soga and Sharif M Mominuzzaman, “Characterization of Electrodeposited Multiwall Carbon Nanotube Films on Silicon Substrates”, 8th International Conference on Electrical and Computer Engineering (ICECE), 2015, 20-22 December 2014, Dhaka, Bangladesh.

[33] Mohammad Rasel Munshi, Md. Torab Hossain, Md. Monohar Hossain, “Opto-electronic Characterization of Nano Carbon Thin Films Deposited on Silicon Substrates” B. Sc. Thesis Department of Electrical and Electronic Engineering, IIUC, Chittagong, Bangladesh, 2015.

[34] Md. Saeed Uddin Mahmud, Md. Moshleh Uddin, Md. Helal Hossain, "Characterization of the Opto-electronic Properties of Carbonic Thin Films Electrodeposited on Zinc Substrates Using Camphoric Methanol Solution" B. Sc. Thesis Department of Electrical and Electronic Engineering, IIUC, Chittagong, Bangladesh, 2008.

[35] The ideal diamond structure, Access date : 24 November, 2021, Retrieved from: https://slideplayer.com/slide/4336038/

[36] Structure of fullerene C 60, Access date : 24 November, 2021, Retrieved from: (13) (PDF) Chronic alcoholization-induced damage to astroglia and intensification of lipid peroxidation in the rat brain: Protector effect of hydrated form of fullerene C60 (researchgate.net)

[37] Some SWNTs with different chiralities. The difference in structure is easily shown at the open end of the tubes. a) armchair structure b) zigzag structure c) chiral structure, Access date : 24 November, 2021, Retrieved from: (13) (PDF) The wondrous world of carbon nanotubes (researchgate.net)

[38] Graphene sheet with vector definitions, Access date : 24 November, 2021, Retrieved from: Microsoft Word - CNT-Afaf-final.doc (ehu.es)

[39] Carbon Nanotubes, Access date : 24 November, 2021, Retrieved from: BandMT_08.pdf (ox.ac.uk)

[40] Mechanical Properties of Carbon Nanotubes, Access date : 24 November, 2021, Retrieved from: 10.1007/3-540-39947-X_12.pdf (springer.com)

[41] Left: A Y-branch, the defects are marked in blue. Right: A transition from a metallic to a semiconducting SWNT. The change is made by insertion of pentagons and heptagons, Access date : 24 November, 2021, Retrieved from: (13) (PDF) The wondrous world of carbon nanotubes (researchgate.net)

[42] Structure of camphor, Access date : 24 November, 2021, Retrieved from: (14) (PDF) Nitrogen and Boron Doped Diamond Like Carbon Thin Films Synthesis by Electrodeposition from Organic Liquids and Their Characterization (researchgate.net)

[43] Touhidul Alam, Md. Shefatullah, K. J. M. Rezaur Rahman, "Characterization of Carbonic Thin Films Electrodeposited on Zn Substrate in Camphoric Methanol Solution" B. Sc. Thesis Department of Electrical and Electronic Engineering, IIUC, Chittagong, Bangladesh, 2011.